

Toward the Frontiers of Particle Physics with the Muon $g-2$ Experiment

Eremey Valetov

Shanghai Jiao Tong University | Michigan State University

On behalf of the Muon $g-2$ Collaboration



上海交通大学
SHANGHAI JIAO TONG UNIVERSITY



李政道研究所
Tsung-Dao Lee Institute

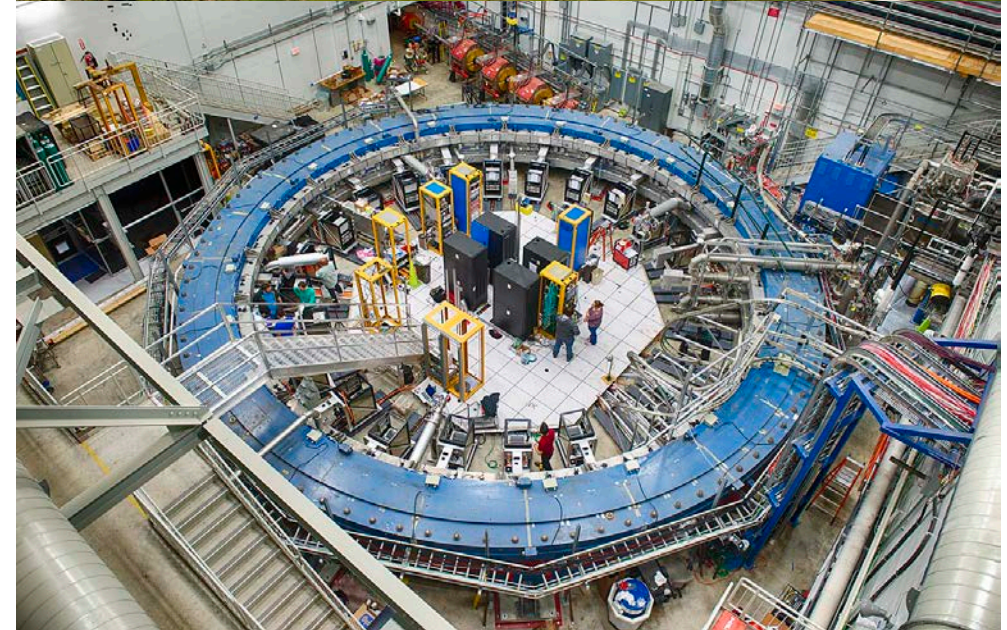
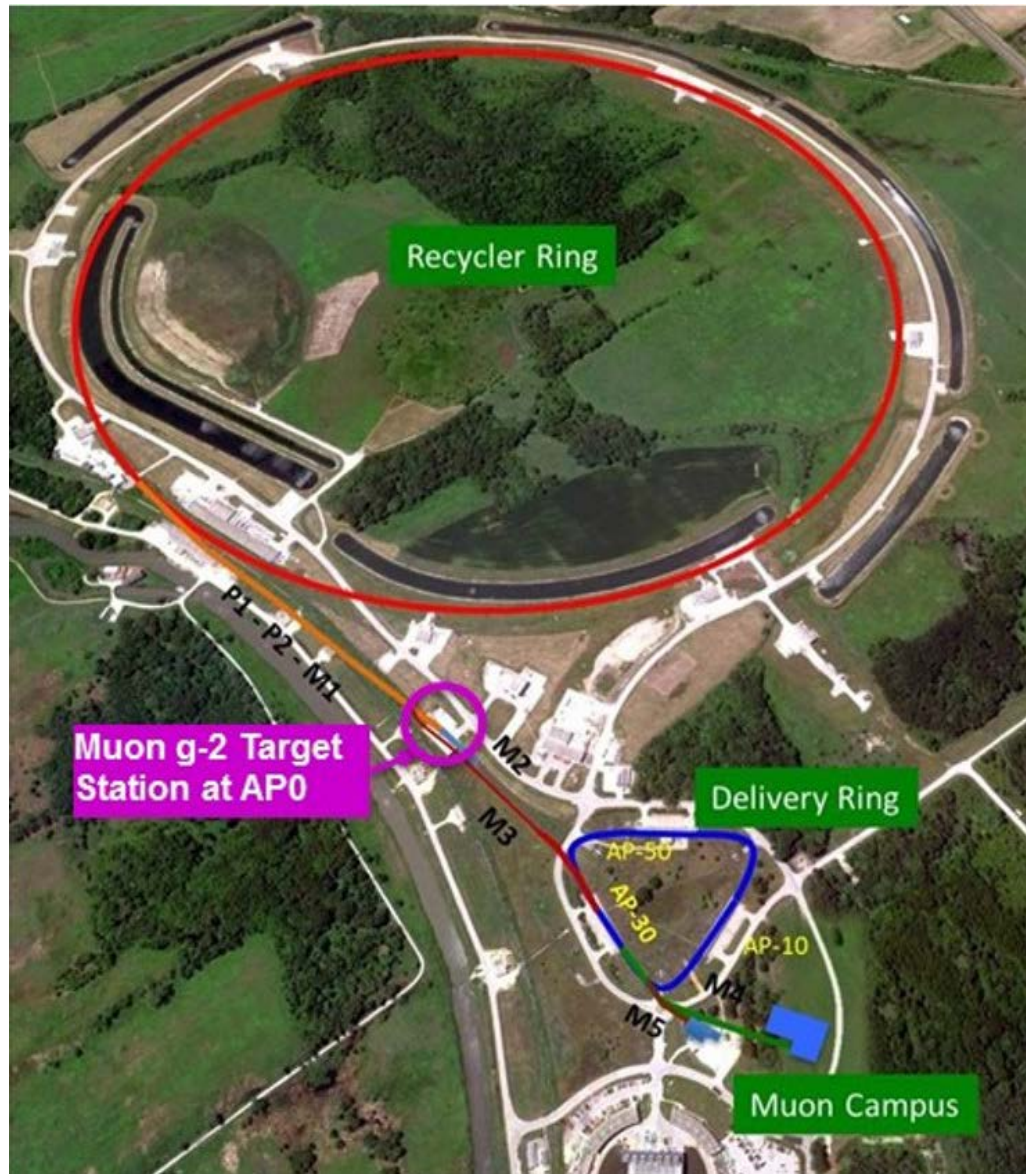
MICHIGAN STATE
UNIVERSITY



U.S. DEPARTMENT OF
ENERGY

Office of
Science

Introduction



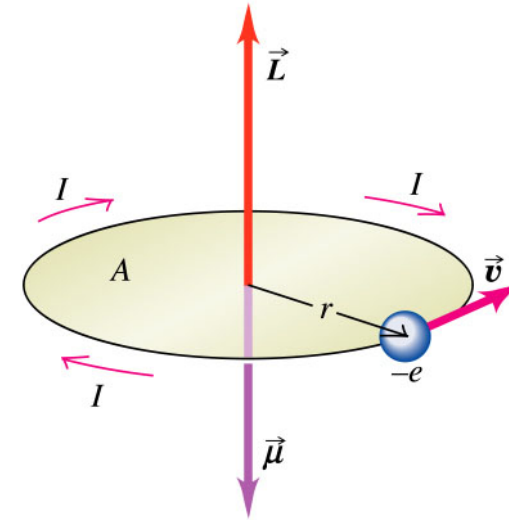
$$\mu = g \frac{e}{2m} s$$

Classical: $g = 1$

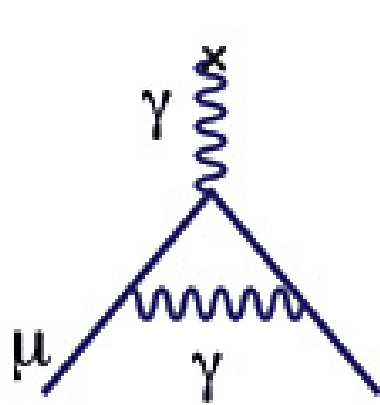
Dirac Equation: $g = 2$

$$i \left(\partial_\mu - ieA_\mu(x) \right) \gamma^\mu \psi(x) = m\psi(x)$$

Interactions w/ quantum foam: $g > 2$ $a_\mu = \frac{g-2}{2}$

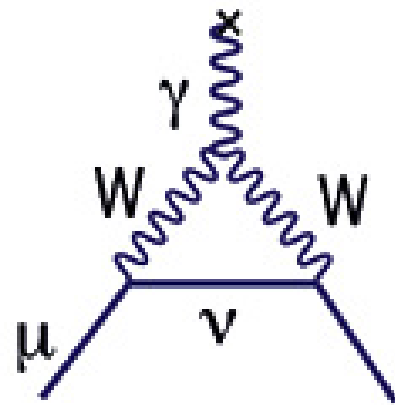


Contributions to a_μ in the Standard Model



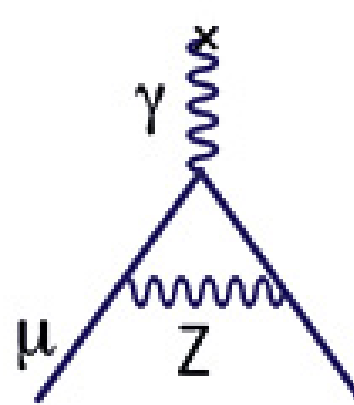
QED

QED incl. 4-loops + 5-loops
 $a_\mu = \mathbf{116\,584\,718.86} \times 10^{-11}$
 $\delta a_\mu = 0.03 \times 10^{-11}$



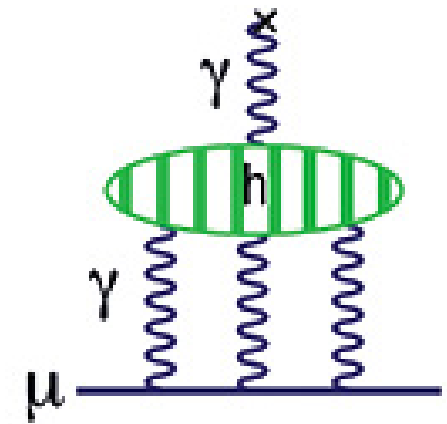
electroweak

Weak to 2-loops
 $a_\mu = 153.6 \times 10^{-11}$
 $\delta a_\mu = 1.1 \times 10^{-11}$



LO hadronic

Hadronic LO VP
 $a_\mu = 6\,894.6 \times 10^{-11}$
 $\delta a_\mu = \mathbf{32.5} \times 10^{-11}$



hadronic LbL

Hadronic LbL
 $a_\mu = 103.4 \times 10^{-11}$
 $\delta a_\mu = \mathbf{28.8} \times 10^{-11}$

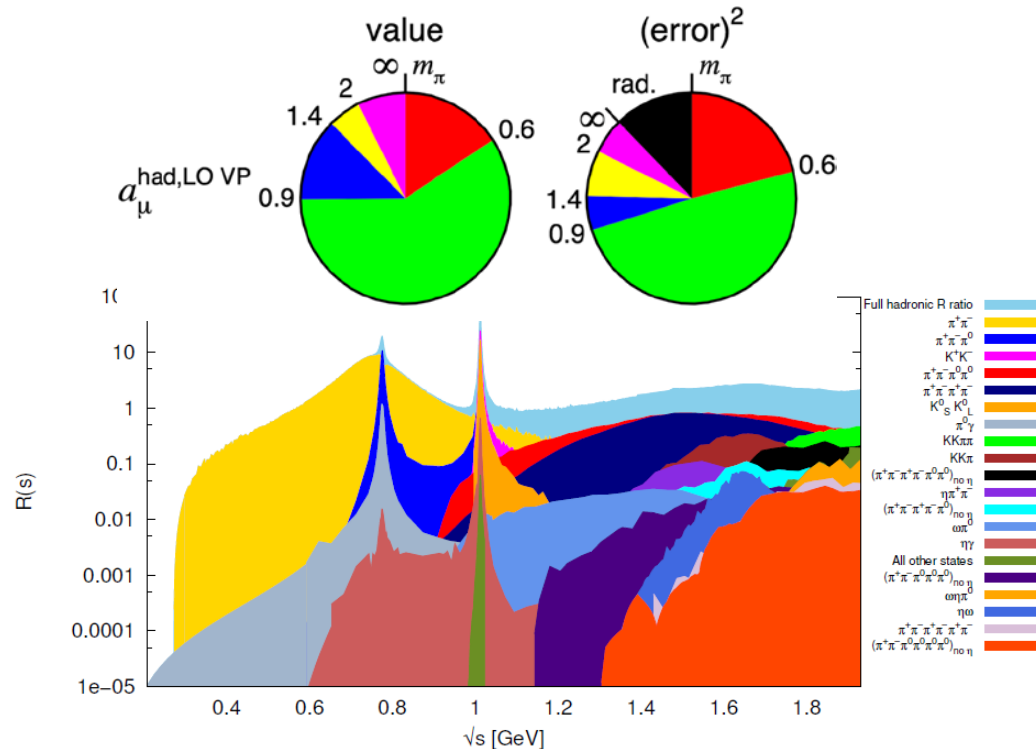
Theory:
 Experiment:

$(11\,659\,1783 \pm 43) \times 10^{-11}$
 $(11\,659\,2091 \pm 63) \times 10^{-11}$

Improvements in $a_\mu^{\text{Had, LO VP}}$ (KNT18)

Direct energy scan: CMD-3, SND, KEDR

Radiative return: BABAR, KLOE/KLOE-2, BESIII

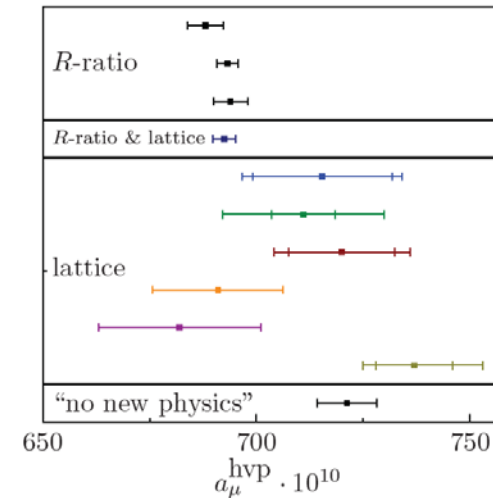


$$a_\mu^{\text{Had, LO VP}} = (693.26 \pm 2.46) \times 10^{-10}$$

A. Keshavarzi, D. Nomura and T. Teubner, Phys. Rev. D **97**, no. 11, 114025 (2018).

Calculation of $a_\mu^{\text{Had, VP}}$ and $a_\mu^{\text{Had, LbL}}$ using Lattice QCD

- From first principles
- Can be used to improve R-ratio results
- Several collaborations working on this
 - including RBC/UKQCD and Mainz
- Precision needs improvement; calculations ongoing



Jegerlehner 2017

Teubner *et al* 2018

Davier *et al* 2019

RBC/UKQCD 2018

RBC/UKQCD 2018

BMW 2017

CLS Mainz 2019

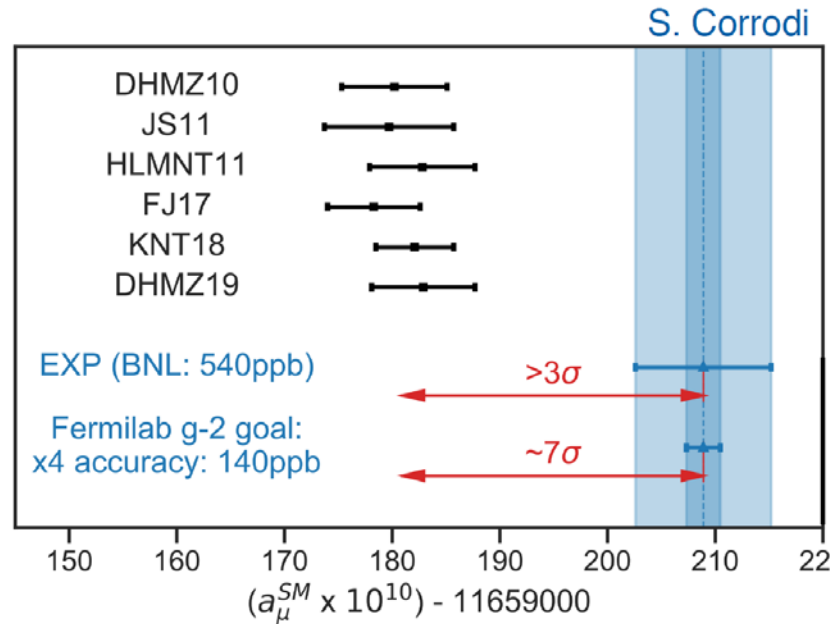
FermiLab/HPQCD/MILC 2019

ETMC 2019

PACS 2019

V. Gülpers, arXiv:2001.11898 [hep-lat] (2020).

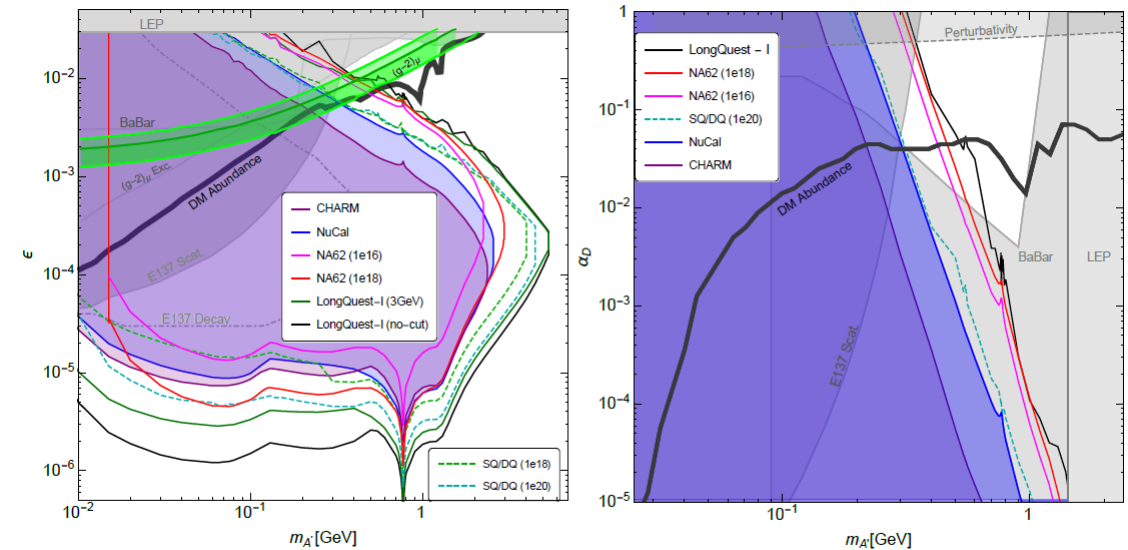
Beyond-Standard Model Possibilities



In case of a Beyond-SM a_μ , some of the possible contributors to the respective discrepancy would be:

- Dark matter
- Supersymmetry (SUSY)
- Extra dimensions
- Additional Higgs Bosons
[S. Iguro *et al.*, arXiv:1907.09845 [hep-ph]]

Muon $g-2$ window in the search for inelastic dark matter (iDM) :

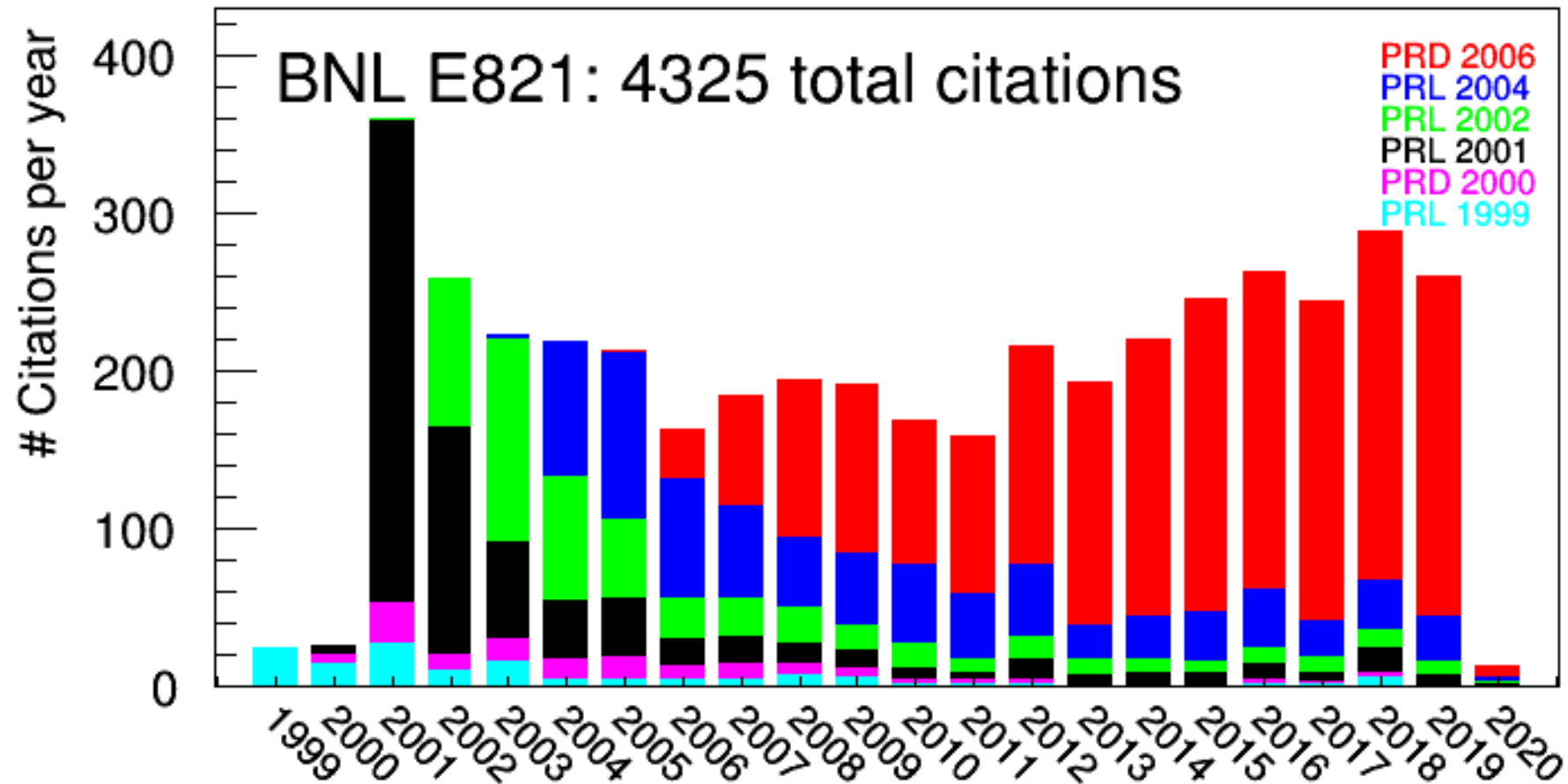


(a_D : analogue of the fine structure constant for a new $U(1)$ gauge symmetry $U(1)_D$. Δ : mass splitting $\Delta = \frac{(m_2 - m_1)}{m_1}$.)

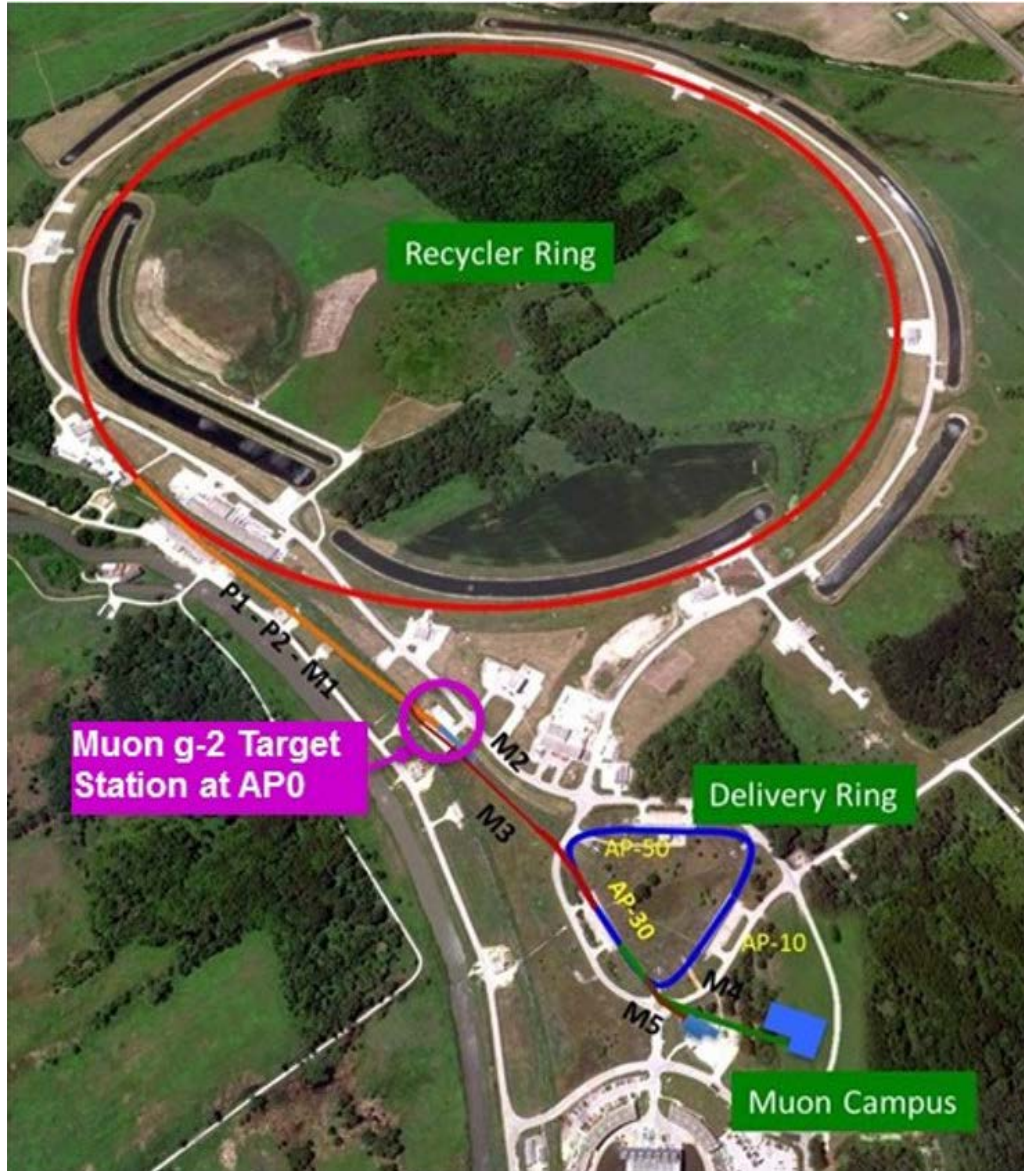
NA62 Experiment at CERN is ongoing and may yield iDM results.

See Y.-D. Tsai *et al.*, arXiv:1908.07525 [hep-ph] (2019).

Citations of Publications of the Muon g-2 Experiment at BNL



The Muon g-2 Experiment at Fermilab (E989)

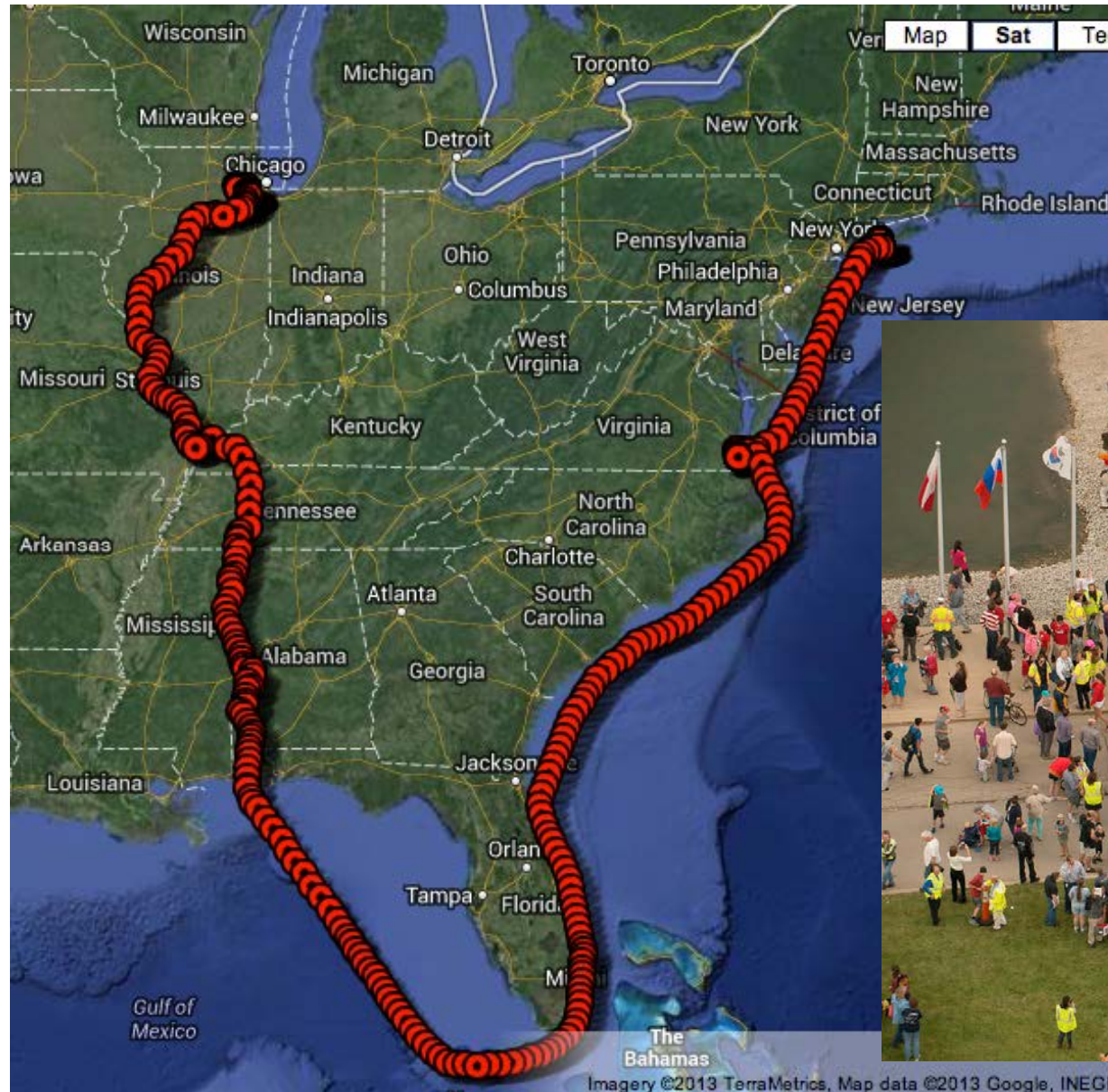


Improvements over the Muon g-2 Experiment at BNL (E821):

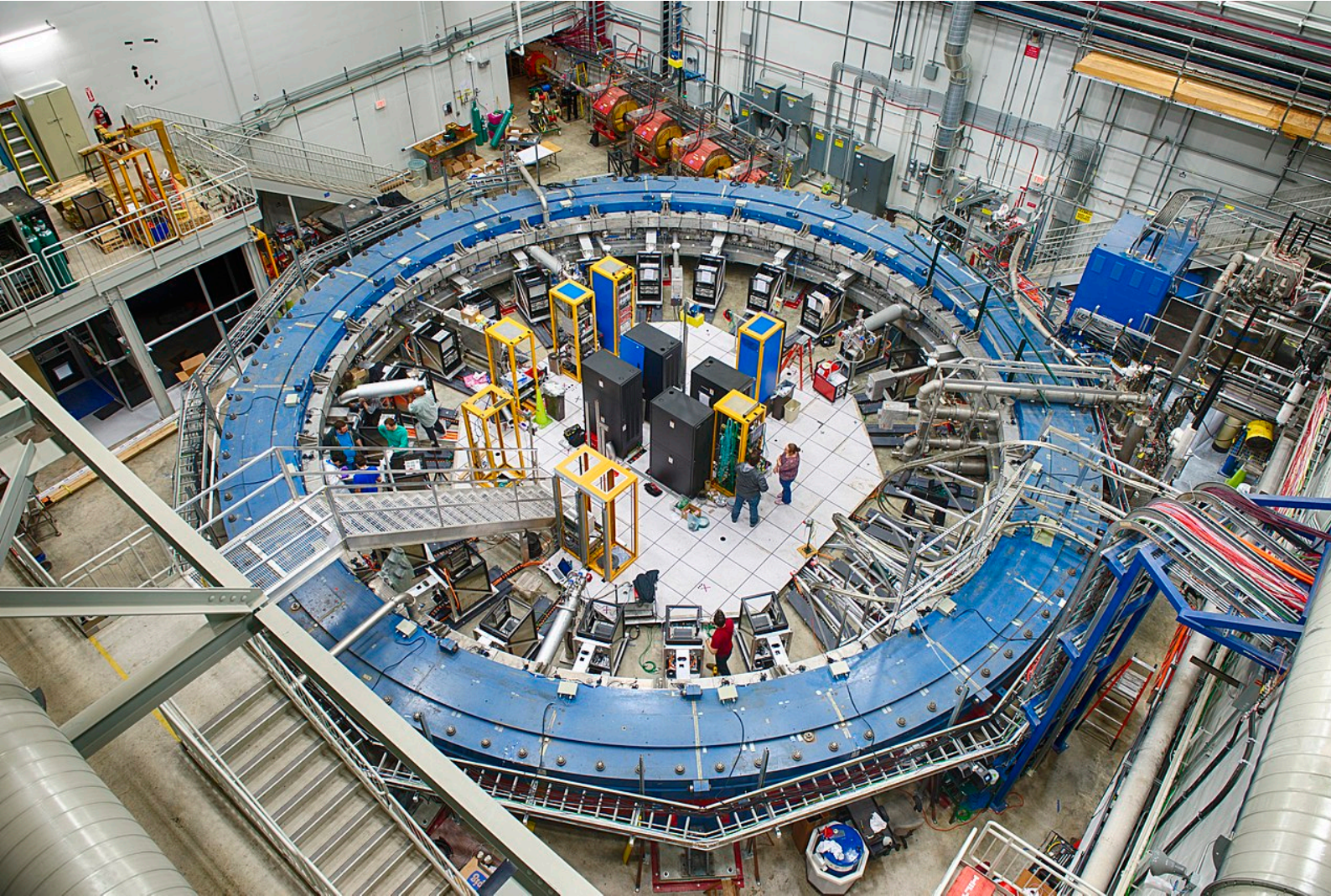
- More muons, delivered more often to the storage ring
- Improved muon storage function
- Better beam dynamics modeling
- Higher field uniformity and better field monitoring
- Reduced spin precession frequency systematics

The Great Move

2013



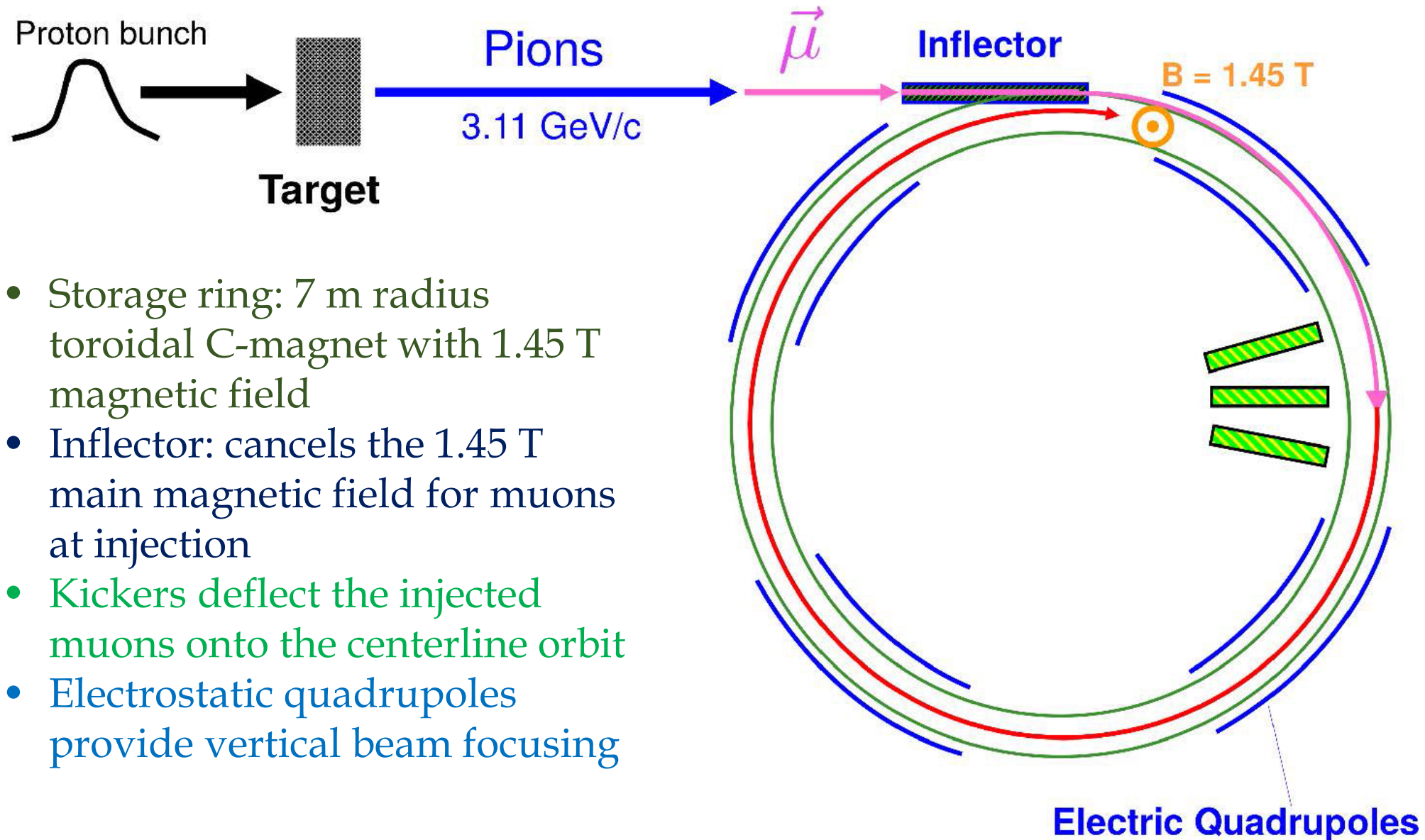
The Muon g-2 Experiment at Fermilab (E989)

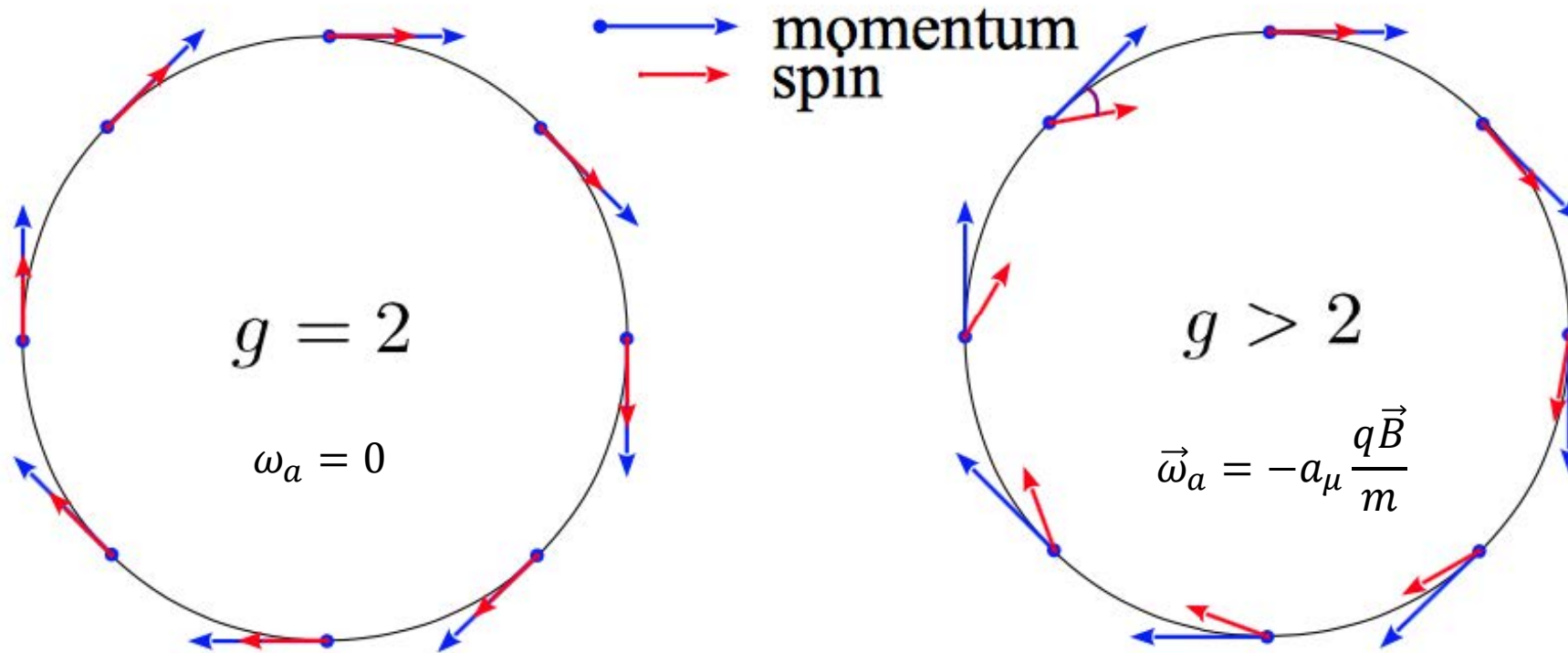


Technical design projection:

- ~20x more data
- ~3x reduction of systematic errors

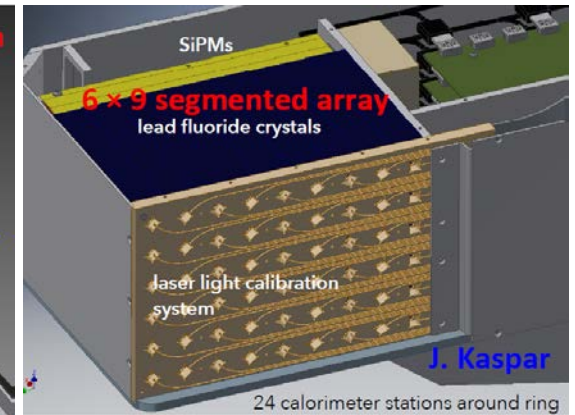
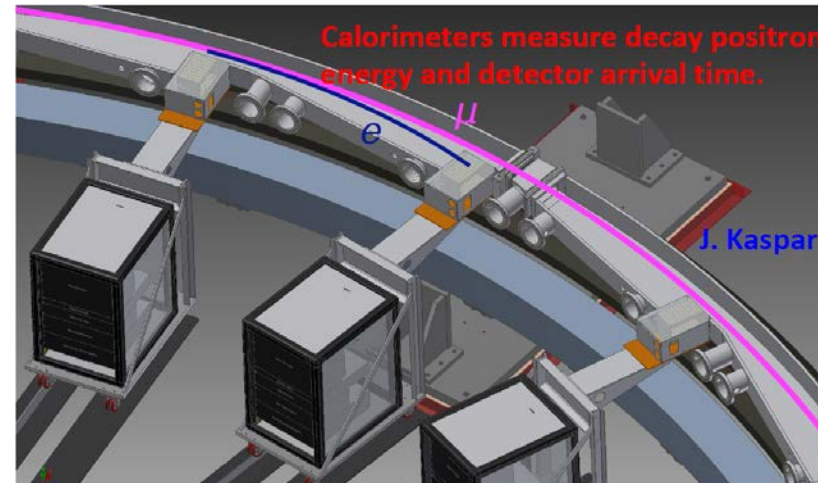
The Muon g-2 Storage Ring



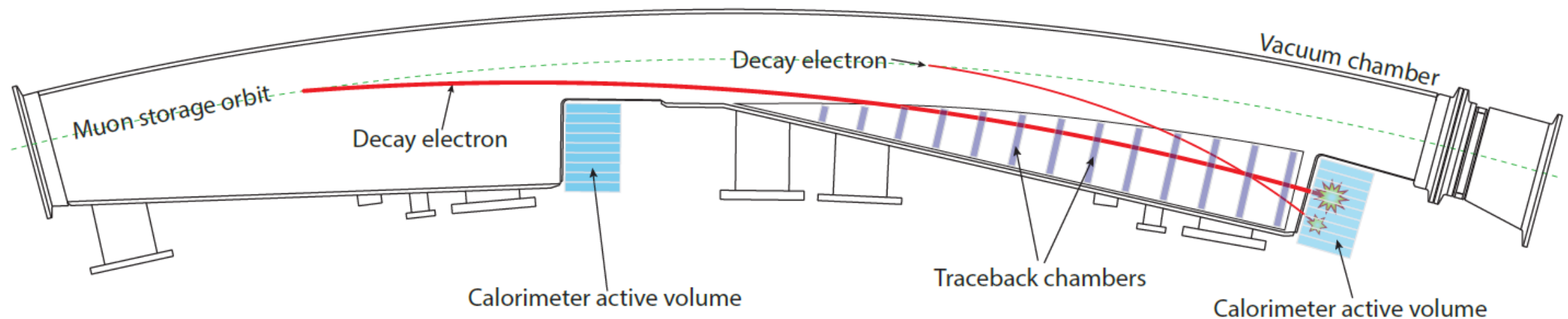


If $g=2$, the angle between the magnetic moment and the momentum does not change.
If $g>2$, the angle between the magnetic moment and the momentum changes linearly.

Measurement of Muon Spin Precession



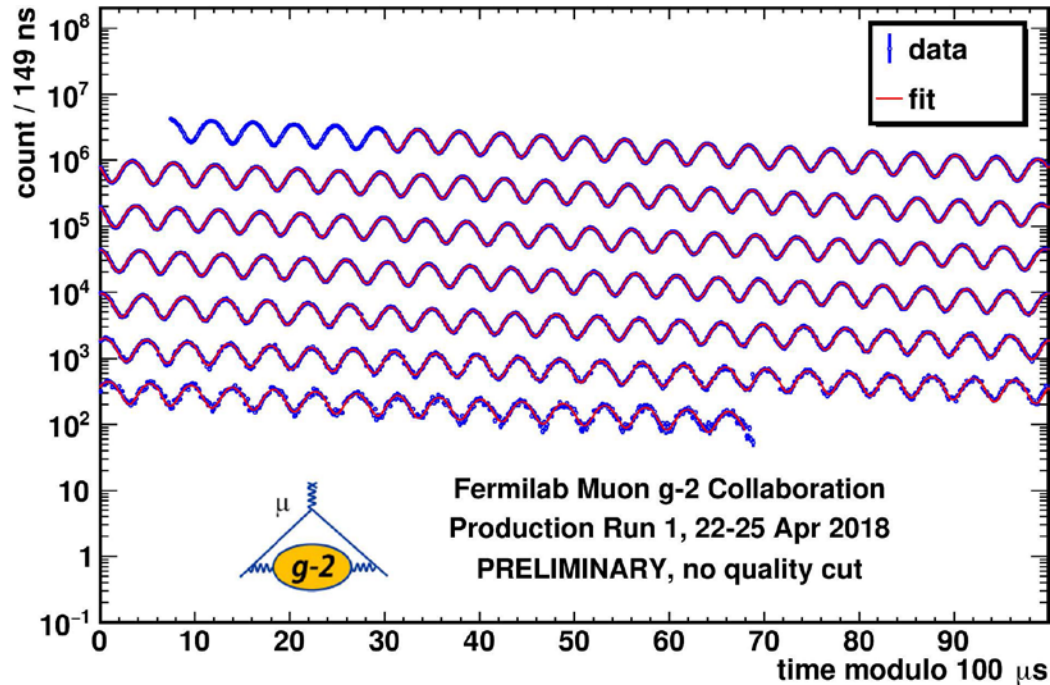
Crystals are 25×25×140 mm



Straw trackers: reconstruct decay e^+ trajectories

Calorimeters: detect decay e^+ energy and arrival times

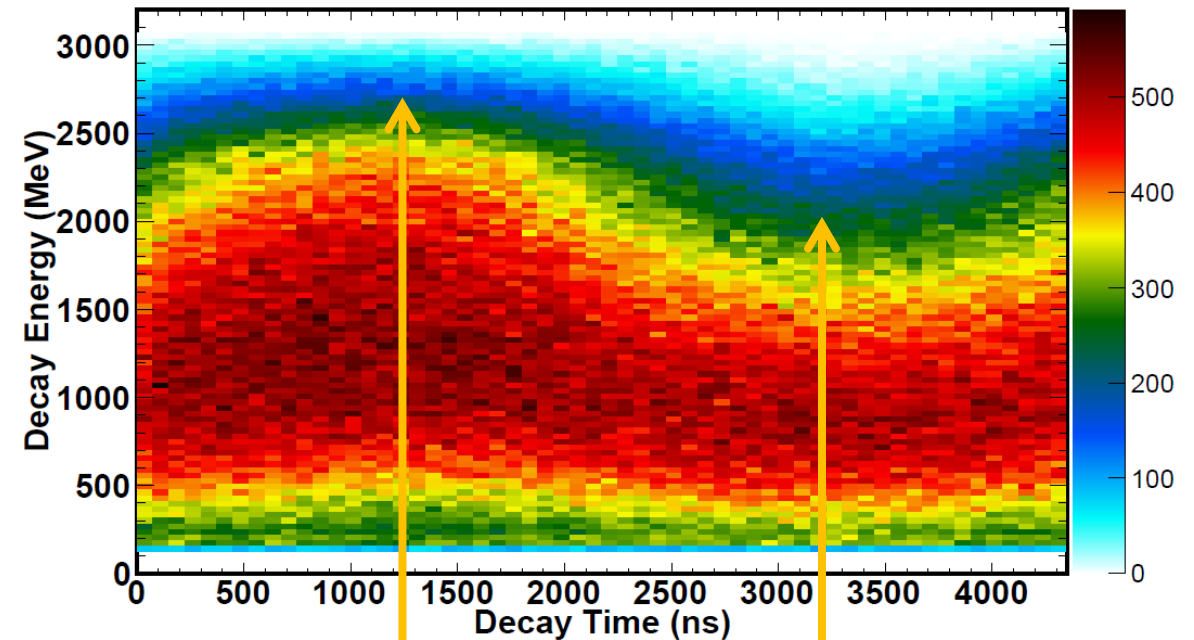
The Wobble Plot



$$f(t) = N_0 e^{-\lambda t} [1 + A \cos(\omega_a t + \phi)]$$

λ : exponential decay constant

ω_a : muon anomalous precession frequency



Muon spin and momentum
are aligned.

Muon spin and momentum
are anti-aligned.

Early-to-late phase change:

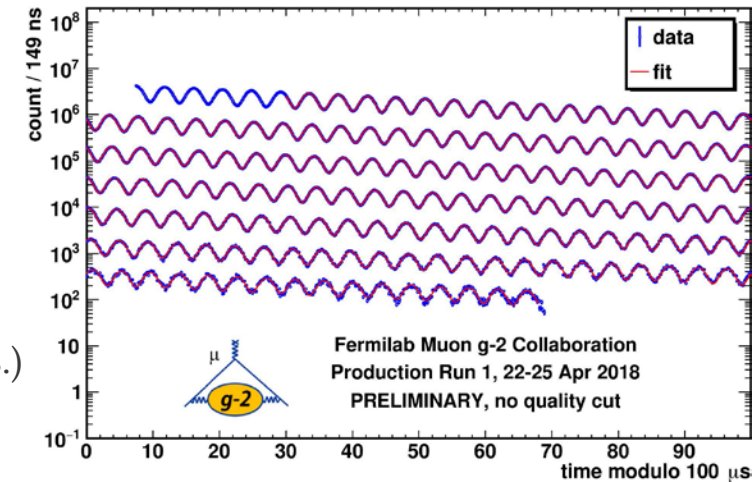
If, $\phi = \phi(t) = \phi_0 + \phi_1 t$, then

$$\begin{aligned} \cos(\omega_a t + \phi) &= \cos(\omega_a t + \phi_0 + \phi_1 t) = \\ &= \cos((\omega_a + \phi_1)t + \phi_0) \end{aligned}$$

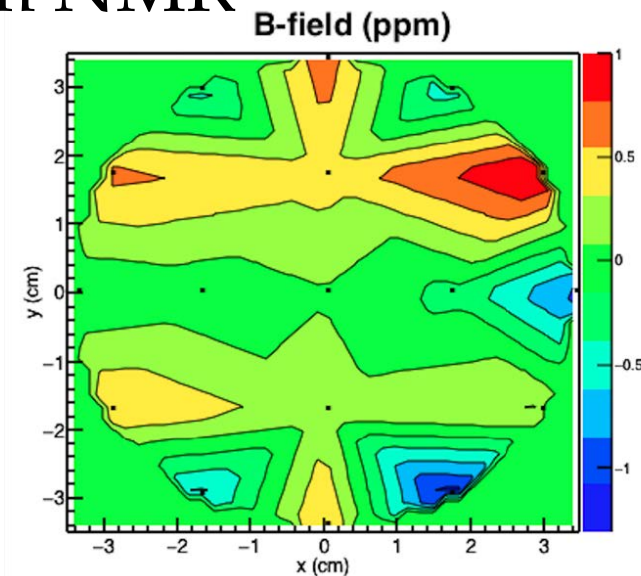
Calculation of a_μ from Muon and Proton Spin Precession

from decay e^+ time spectra

$$a_\mu = \frac{\frac{g_e}{2} \frac{m_\mu}{m_e} \omega_a}{\left\langle \omega_p \right\rangle \frac{\mu_e}{\mu_p}} \quad \begin{array}{l} (140 \text{ ppb}) \\ (70 \text{ ppb sys.} \\ 100 \text{ ppb stat.}) \\ (70 \text{ ppb sys.}) \end{array}$$



from NMR



From CODATA [1]:

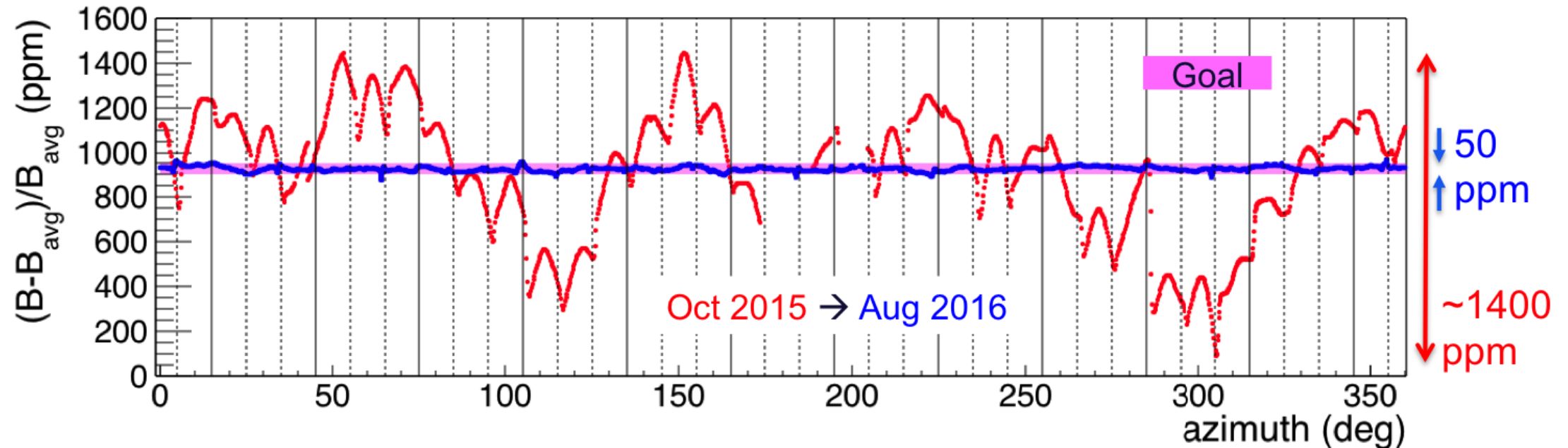
$$g_e = -2.002\,319\,304\,361\,82(52) \text{ (0.00026 ppb)}$$

$$m_\mu/m_e = 206.768\,2826(46) \text{ (22 ppb)}$$

$$\mu_e/\mu_p = -658.210\,6866(20) \text{ (3.0 ppb)}$$

[1] P. J. Mohr, D. B. Newell and B. N. Taylor, Rev. Mod. Phys. 88, no. 3, 035009 (2016).

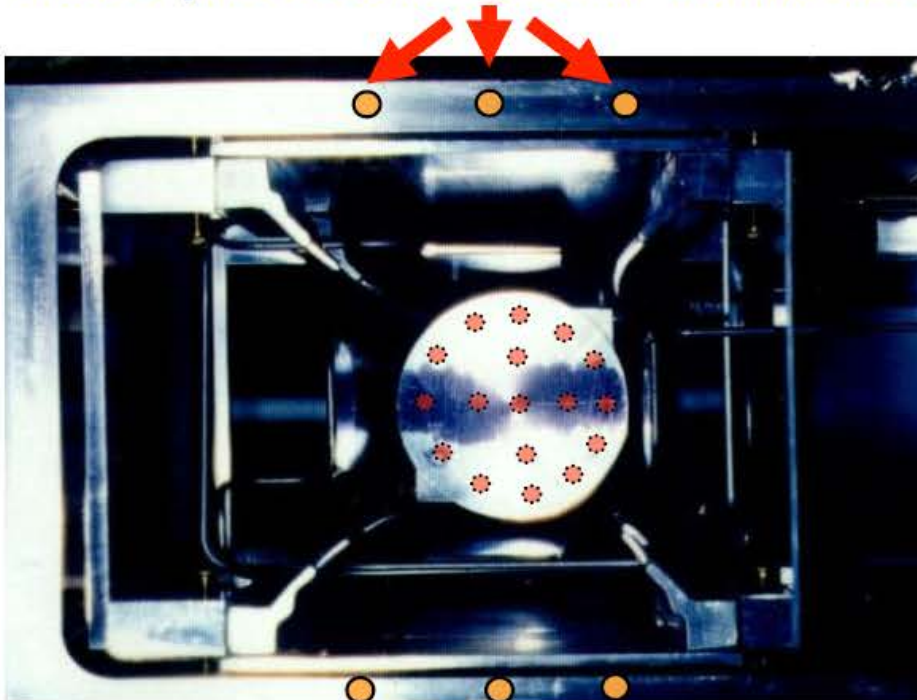
Magnetic Field Shimming



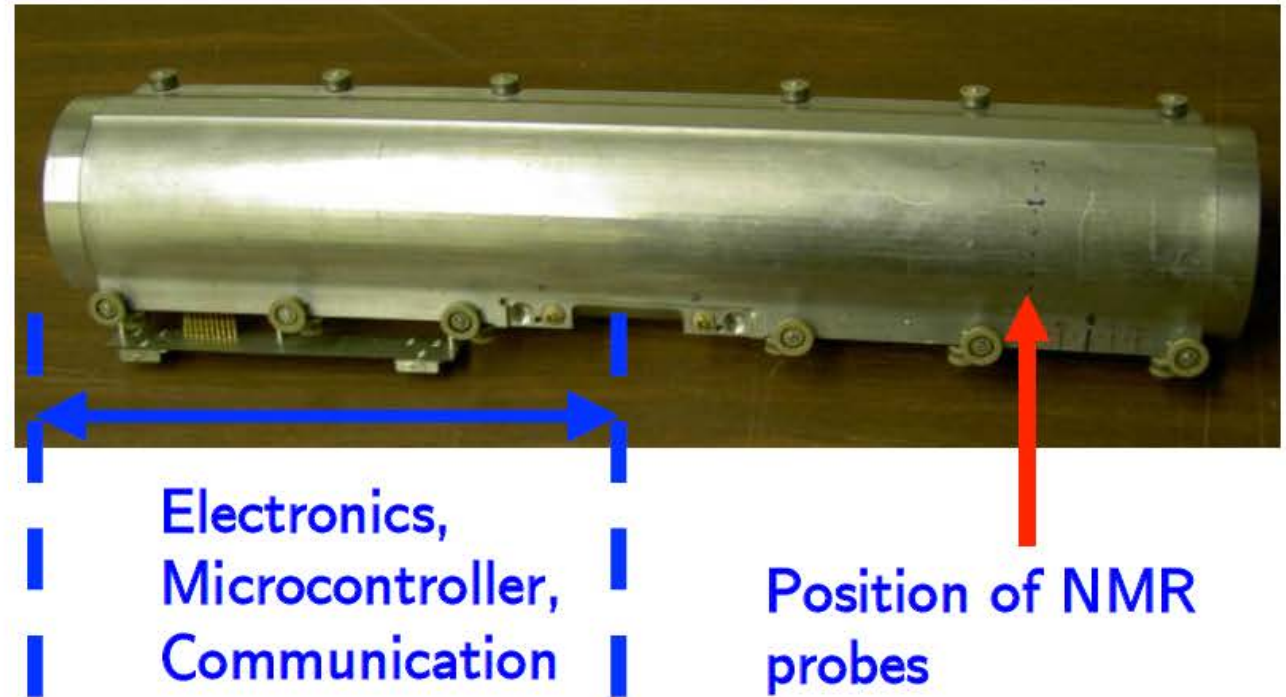
- Passive shimming is performed by inserting tiny metal pieces to increase the field.
- Magnetic field was made 3x more uniform than at BNL.
- Active shimming is also used.

Fixed and Trolley-Mounted NMR Probes

Fixed probes on vacuum chambers



Trolley with matrix of 17 NMR probes



ω_a Systematics

Table 5.2: The largest systematic uncertainties for the final E821 ω_a analysis and proposed upgrade actions and projected future uncertainties for data analyzed using the T method. The relevant Chapters and Sections are given where specific topics are discussed in detail.

| Category | E821 [ppb] | E989 Improvement Plans | Goal [ppb] | Chapter & Section |
|---------------|------------|----------------------------------|------------|-------------------|
| Gain changes | 120 | Better laser calibration | 20 | 16.3.1 |
| Pileup | 80 | Low-energy samples recorded | 40 | 16.3.2 |
| Lost muons | 90 | calorimeter segmentation | 20 | 13.10 |
| CBO | 70 | Better collimation in ring | < 30 | 13.9 |
| E and pitch | 50 | Higher n value (frequency) | 30 | 4.4 |
| | | Better match of beamline to ring | | |
| | | Improved tracker | | |
| | | Precise storage ring simulations | | |
| Total | 180 | Quadrature sum | 70 | |

We will consider the lost muons systematic error in some detail later in this presentation.

ω_p Systematics

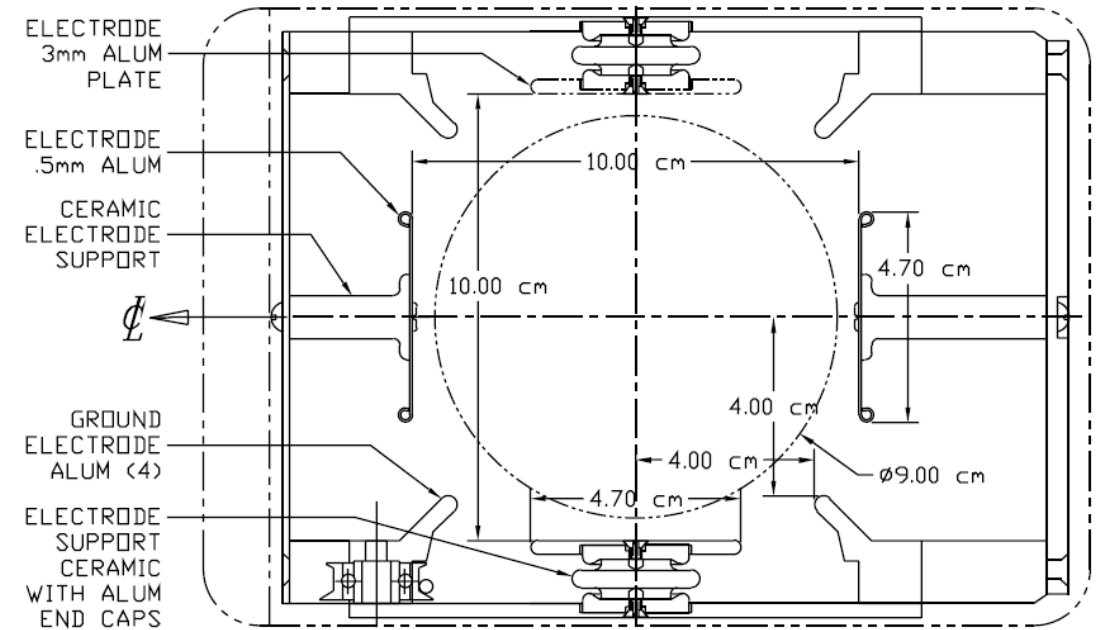
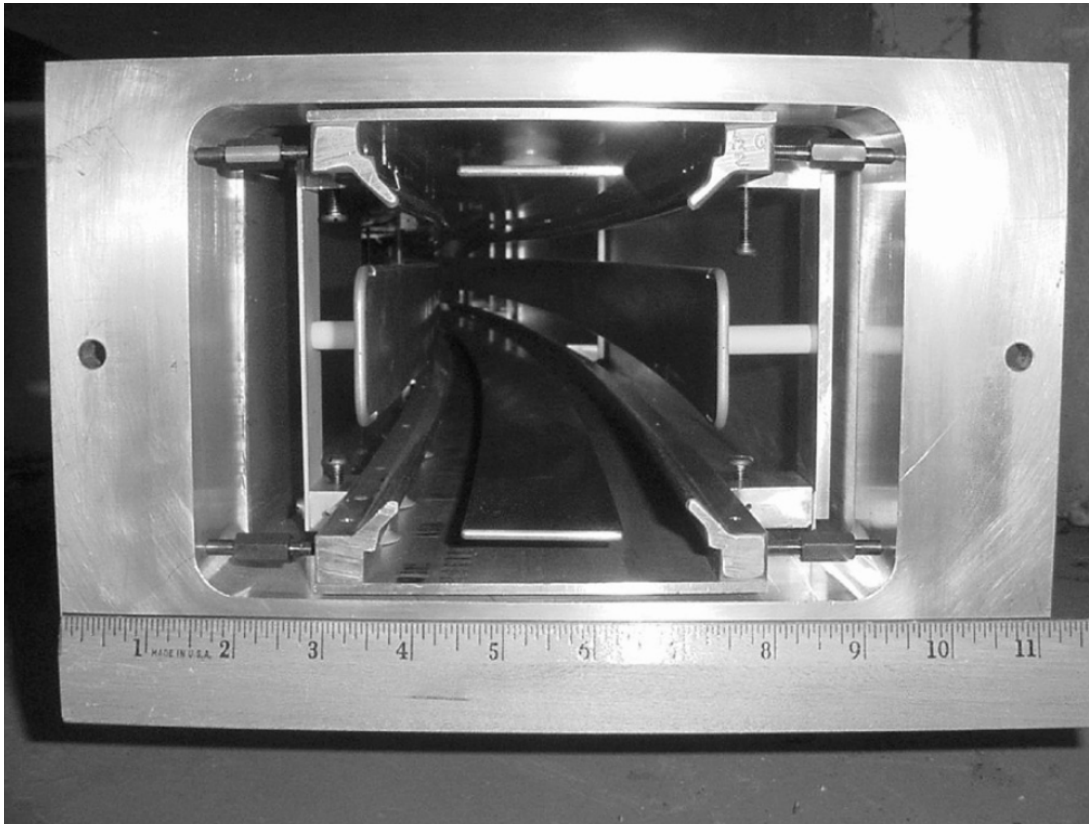
Table 5.3: Systematic uncertainties estimated for the magnetic field, ω_p , measurement. The final E821 values are given for reference, and the proposed upgrade actions are projected. Note, several items involve ongoing R&D, while others have dependencies on the uniformity of the final shimmed field, which cannot be known accurately at this time. The relevant Chapters and Sections are given where specific topics are discussed in detail.

| Category | E821 [ppb] | Main E989 Improvement Plans | Goal [ppb] | Chapter |
|---|------------|---|------------|---------|
| Absolute field calibration | 50 | Special 1.45 T calibration magnet with thermal enclosure; additional probes; better electronics | 35 | 15.4.1 |
| Trolley probe calibrations | 90 | Plunging probes that can cross calibrate off-central probes; better position accuracy by physical stops and/or optical survey; more frequent calibrations | 30 | 15.4.1 |
| Trolley measurements of B_0 | 50 | Reduced position uncertainty by factor of 2; improved rail irregularities; stabilized magnet field during measurements* | 30 | 15.3.1 |
| Fixed probe interpolation | 70 | Better temperature stability of the magnet; more frequent trolley runs | 30 | 15.3 |
| Muon distribution | 30 | Additional probes at larger radii; improved field uniformity; improved muon tracking | 10 | 15.3 |
| Time-dependent external magnetic fields | – | Direct measurement of external fields; simulations of impact; active feedback | 5 | 15.6 |
| Others † | 100 | Improved trolley power supply; trolley probes extended to larger radii; reduced temperature effects on trolley; measure kicker field transients | 30 | 15.7 |
| Total systematic error on ω_p | 170 | | 70 | 15 |

In the following eight or nine slides, I will talk about some of my personal contributions:

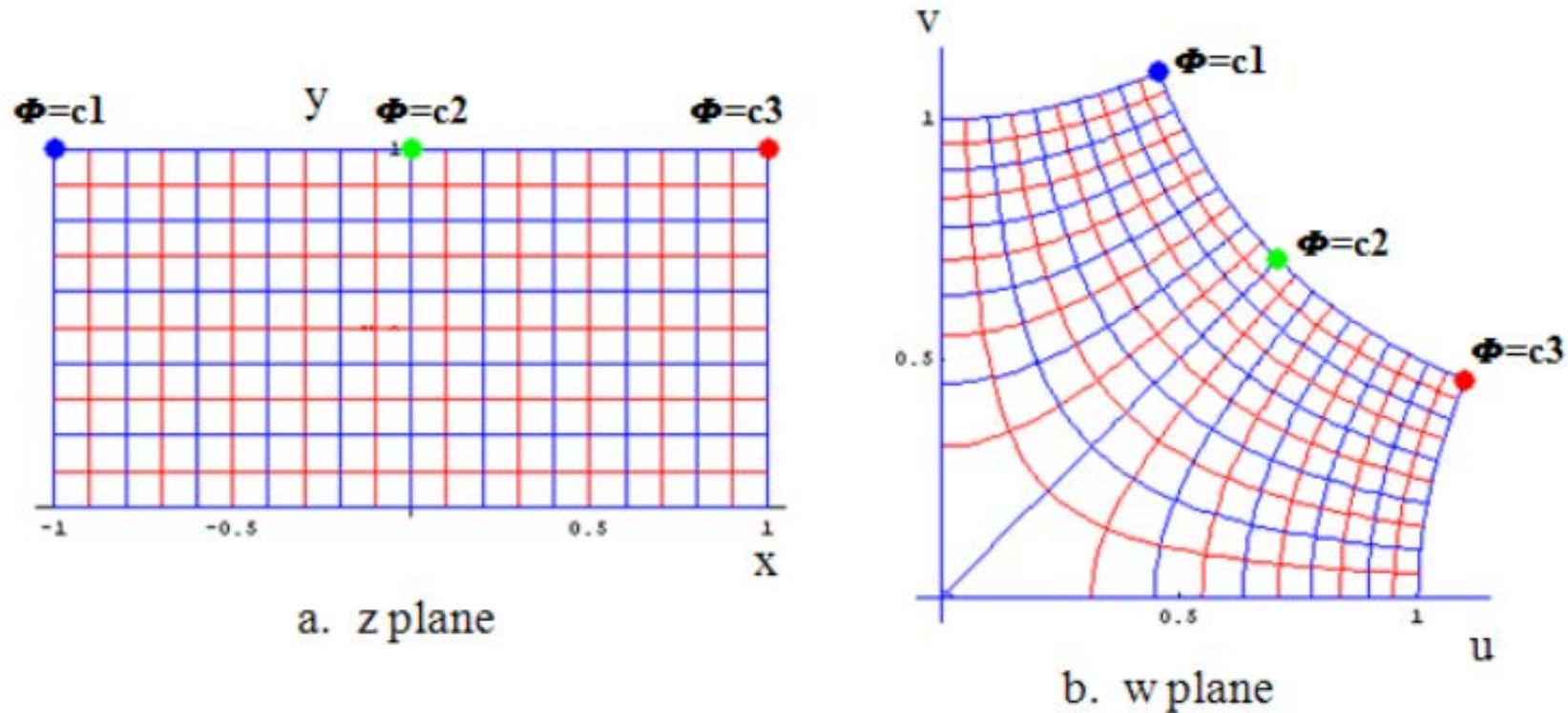
- field calculation for quads*
- end-to-end simulations*
- application of simulation results to muon loss systematics*

Muon g-2 Storage Ring High Voltage Quadrupoles



ELECTRODE AND SUPPORT FRAME - END VIEW

Conformal Mapping Methods



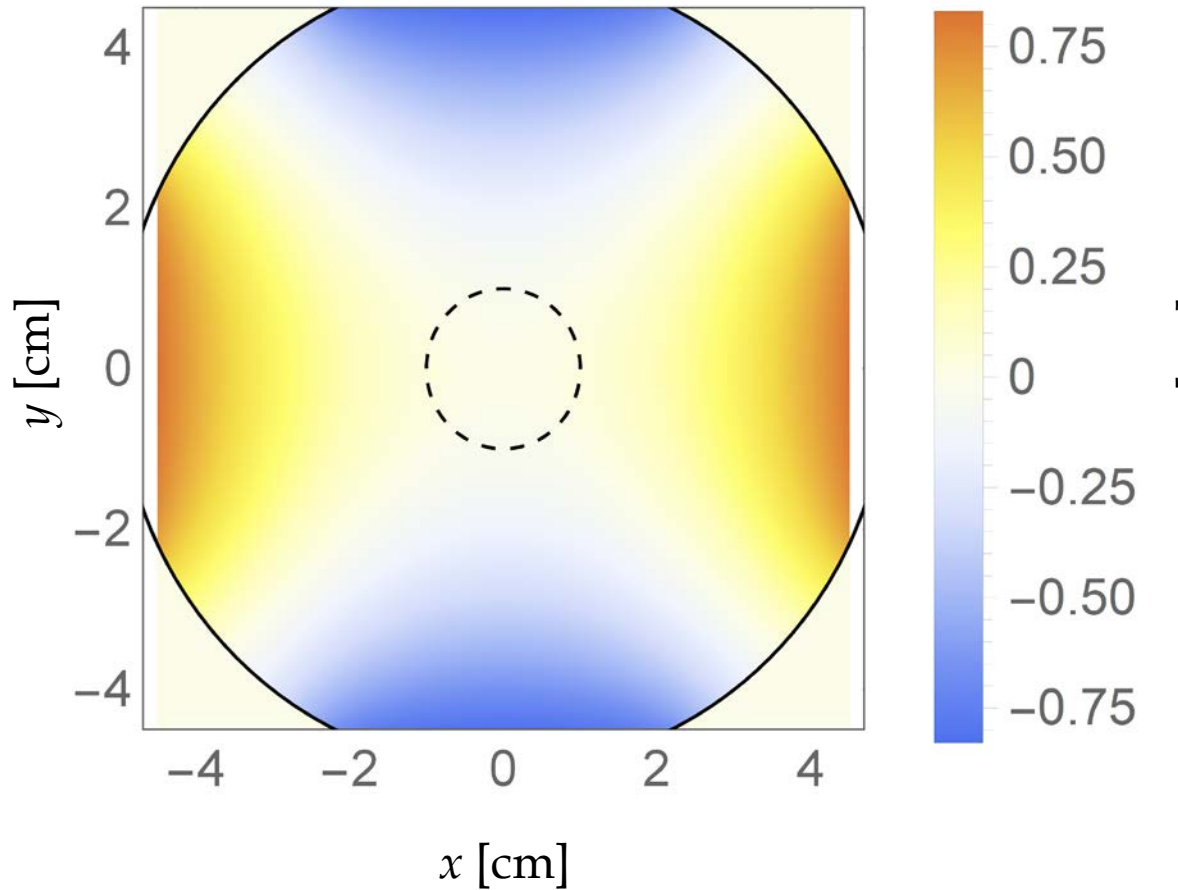
$$f'(z) = c \operatorname{cn}(z|m) \operatorname{dn}(z|m) \prod_{j=1}^n (\operatorname{sn}(z|m) - \operatorname{sn}(x_j + iy_j|m))^{\alpha_j - 1}$$

Advantages of conformal mappings for field calculations:

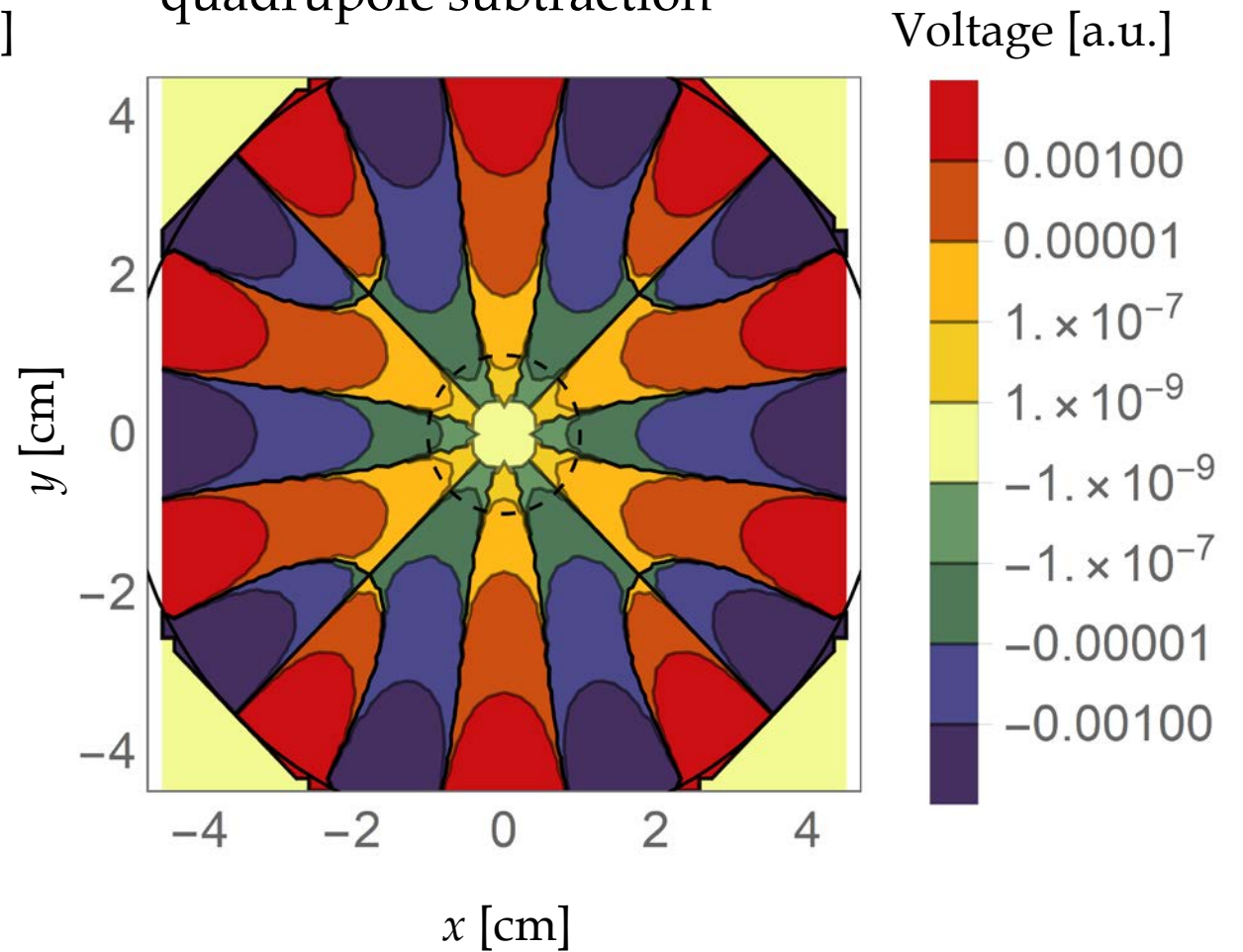
- Fully Maxwellian
- Rapid recalculations with voltage asymmetries (e.g. for RF scraping)

Multipole Expansion of the Quadrupole Potential

Field dominated by quadrupole moment

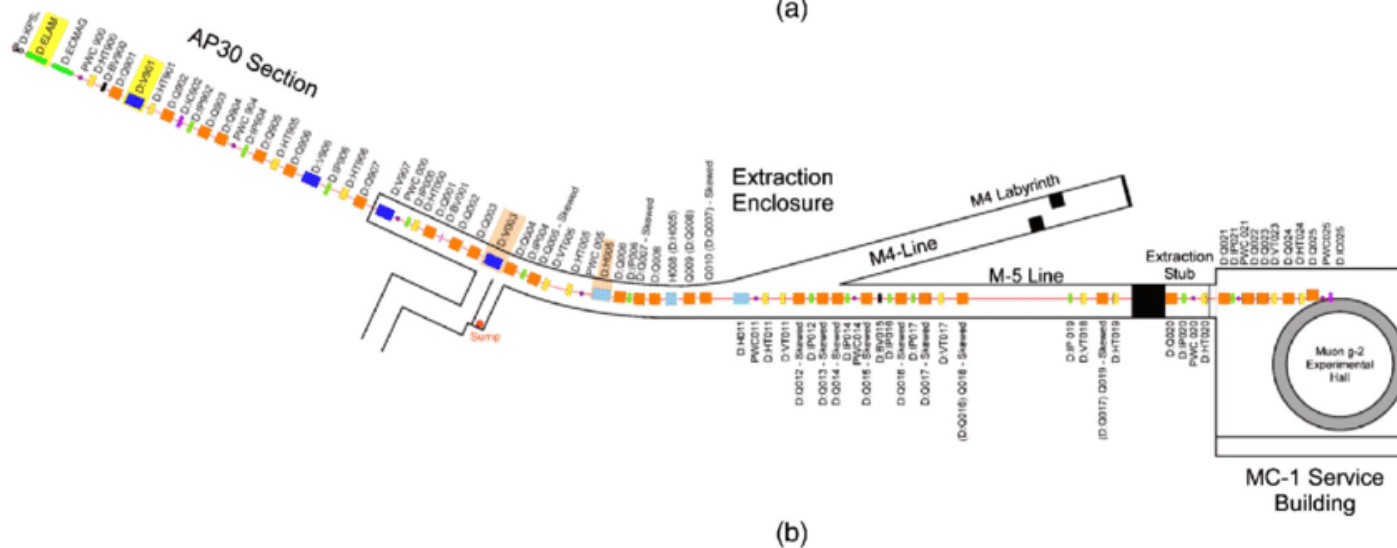


Higher order multipoles after quadrupole subtraction

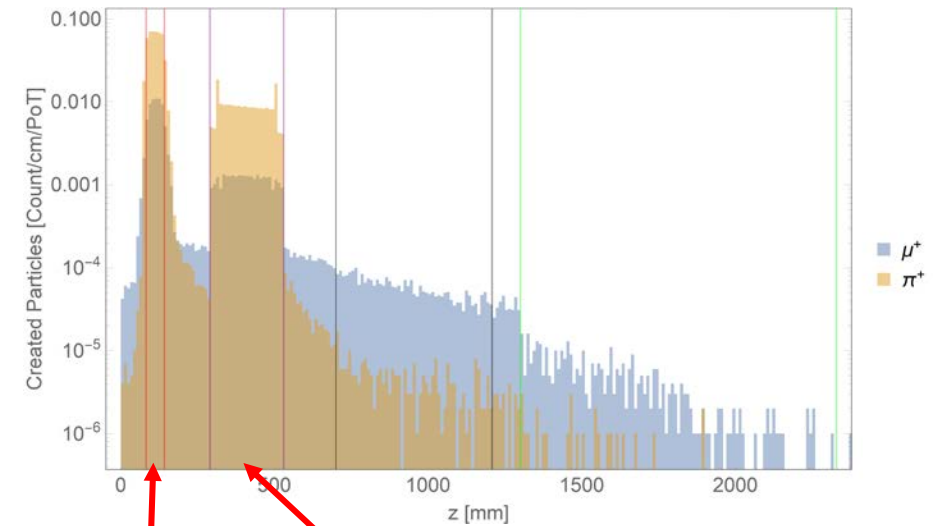
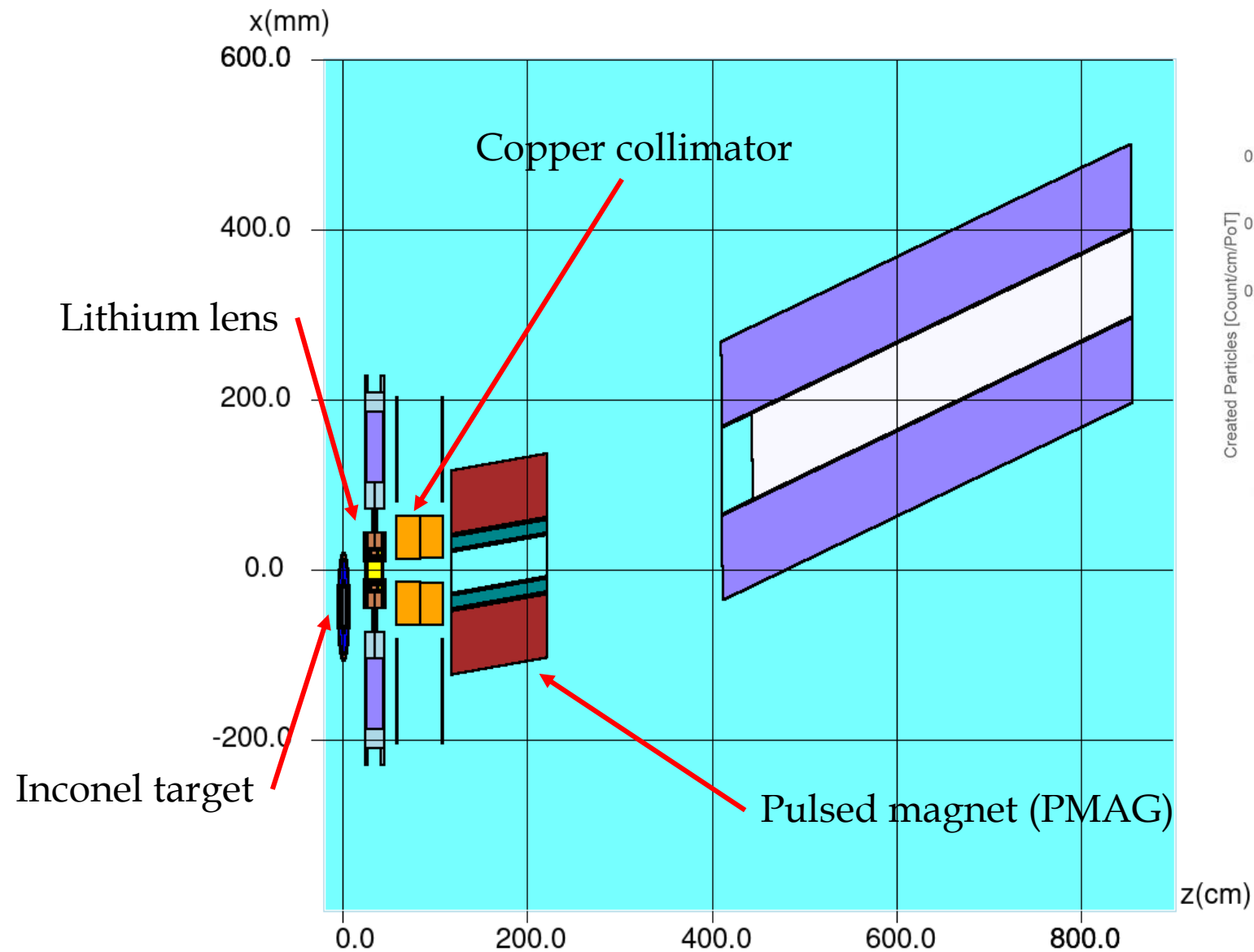




Need to understand potential sources of early-to-late beam-related systematics.



Muon g-2 Target Station



Target

Lithium Lens

Simulations Using High Performance Computing Systems



2×10^{13} protons
on target

HPC systems:

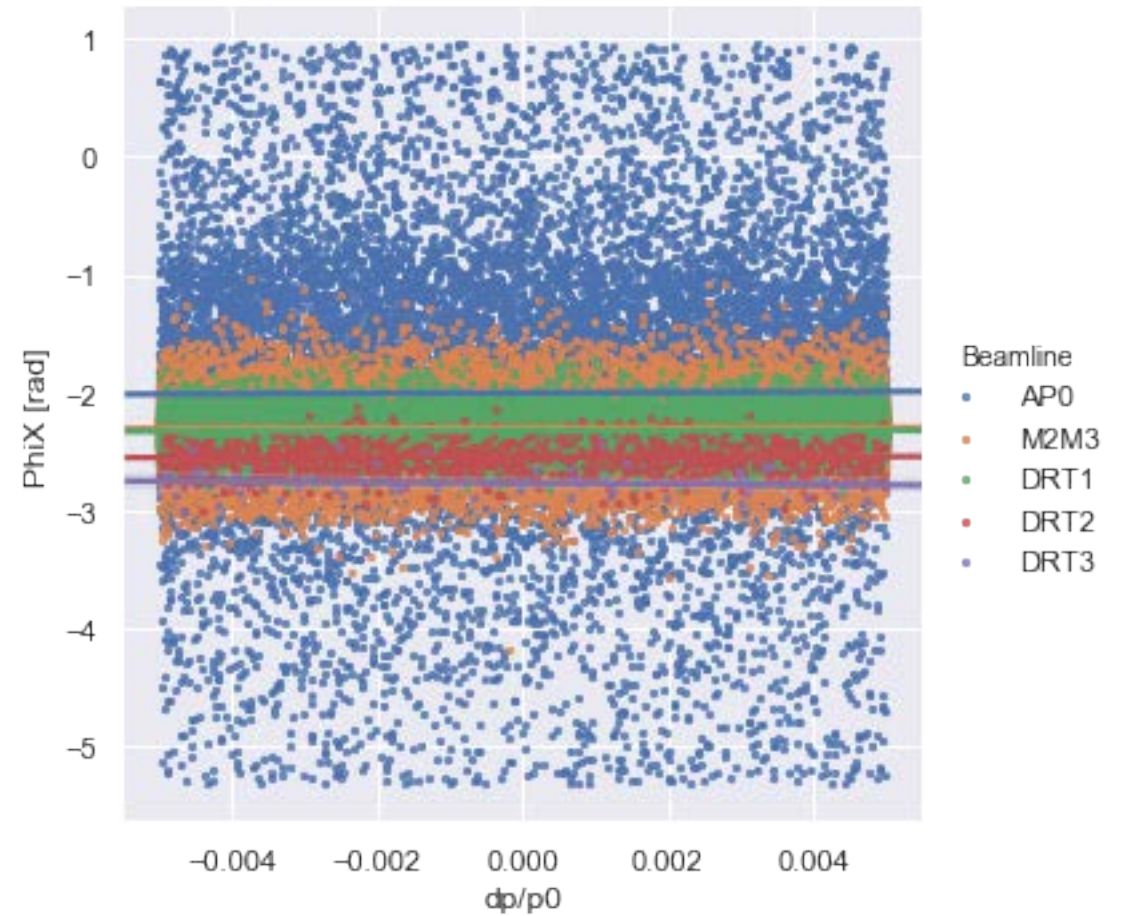
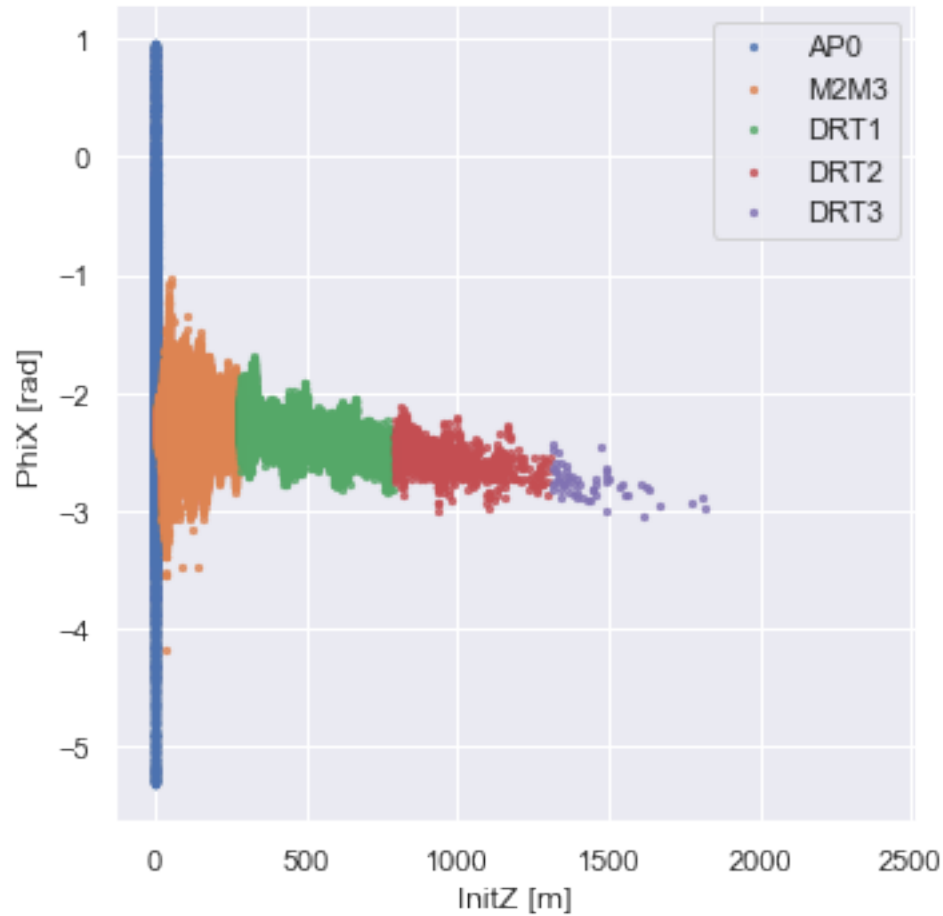
- NERSC
 - Edison (2013–2019):
2.57 PFLOPS
 - Cori (2015–):
30 PFLOPS
- Open Science Grid
 - Up to 10000 cores
at a time
- FermiGrid

Simulation tools:

- gm2ringsim (Geant4)
- COSY INFINITY
- BMAD
- MARS
- G4Beamline (Geant4)

Dependence of Initial Phase on Muon Creation Location

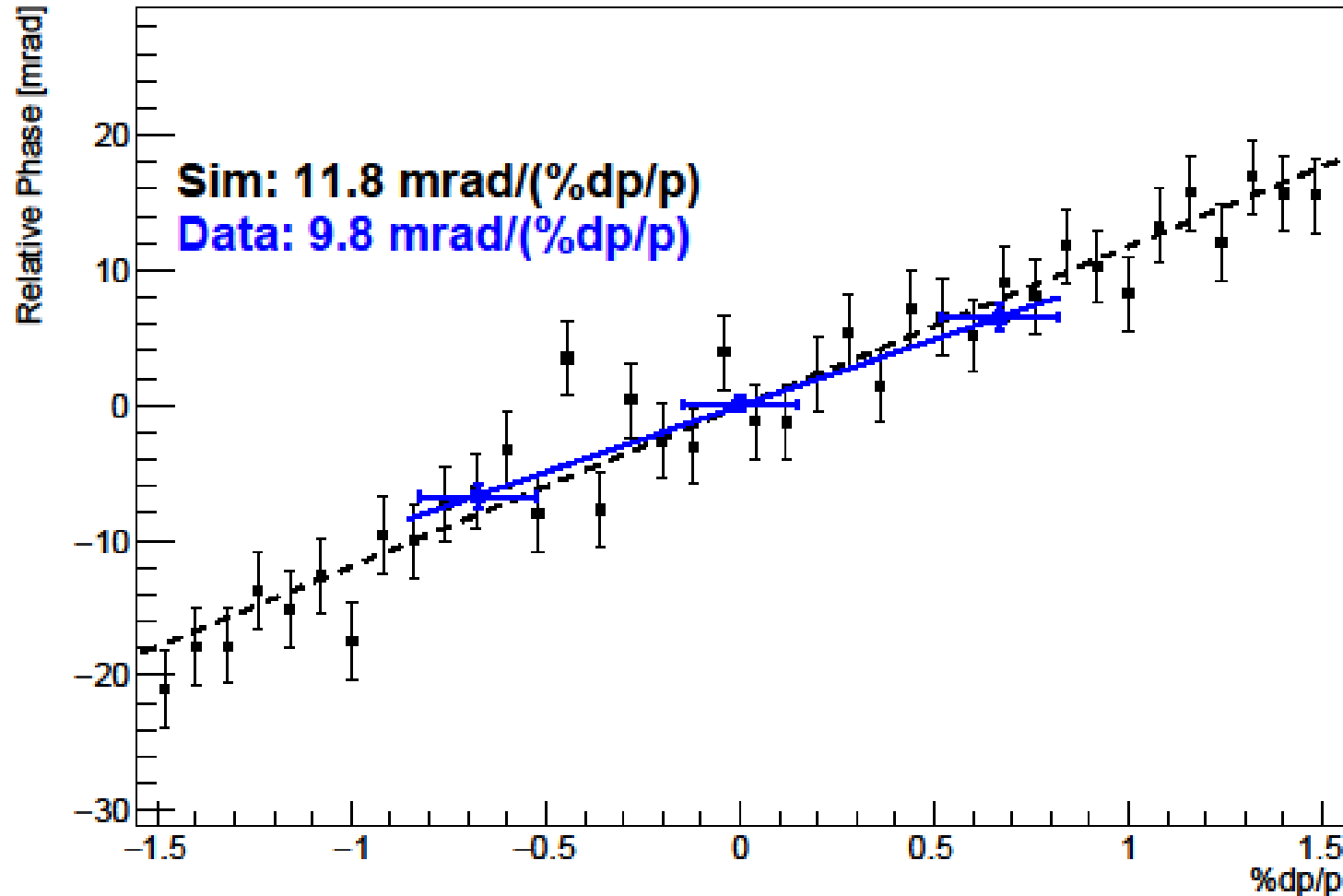
Simulation results, preliminary



InitZ : muon creation location. Φ_X : muon spin phase at entrance into the ring. dp/p_0 : momentum deviation.
All data within $\left| \frac{dp}{dp_0} \right| < 0.5\%$, i.e. 3σ acceptance of the storage ring.

Dependence of Relative Initial Phase on Momentum

Preliminary. Experimental data: Hannah Binney.

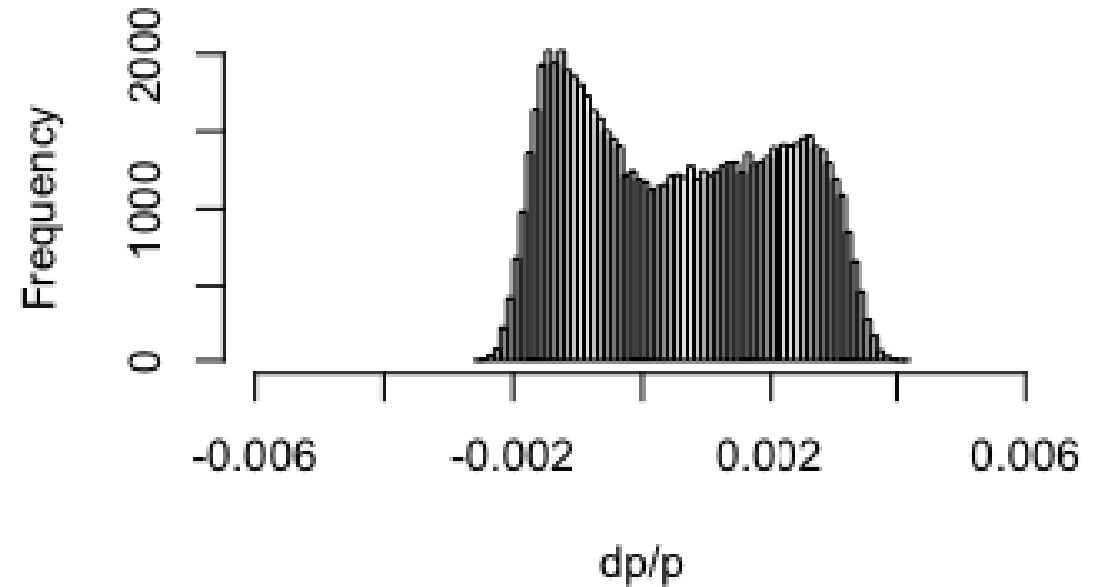
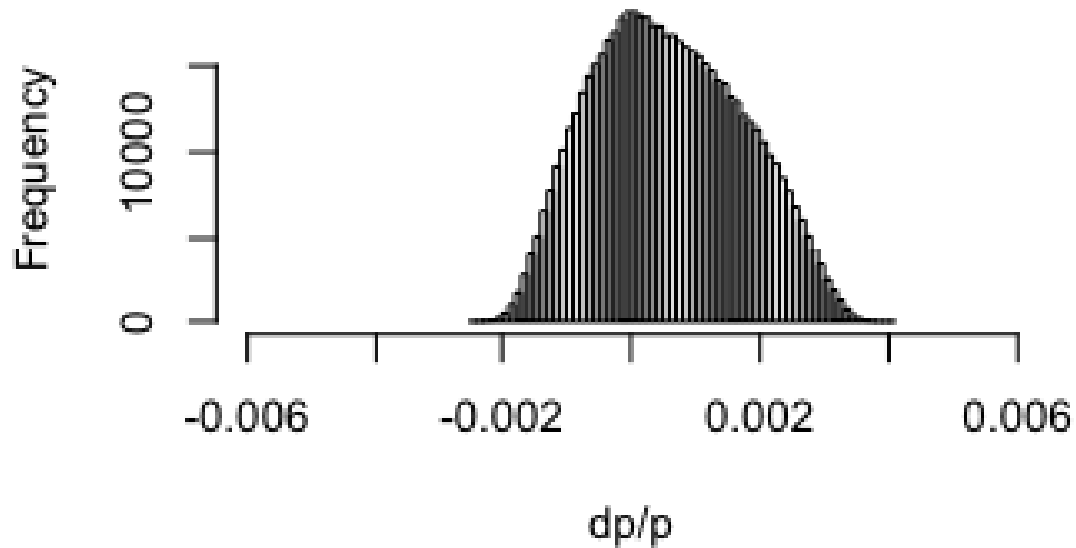


A real momentum dependence of the initial phase develops because of magnetic dipoles in the Delivery Ring.

Experimental data: based on runs with muon storage with higher or lower momenta.

Momentum-Dependent Muon Losses

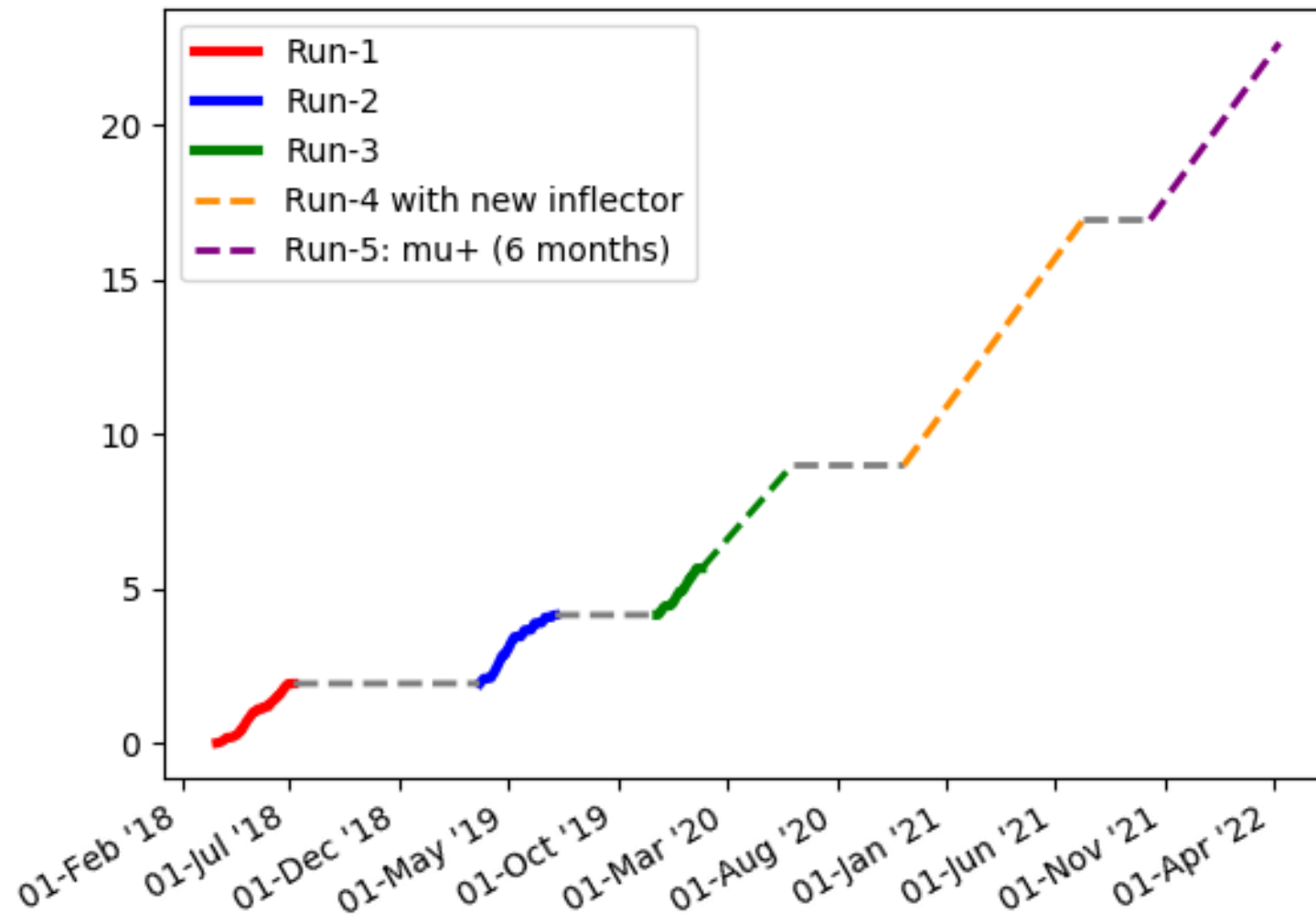
Simulation results, preliminary (Mike Syphers)



Work is still in progress, but we expect a 10-20 ppb error due to muon losses. Far below the overall 70 ppb systematic error on the spin precession.

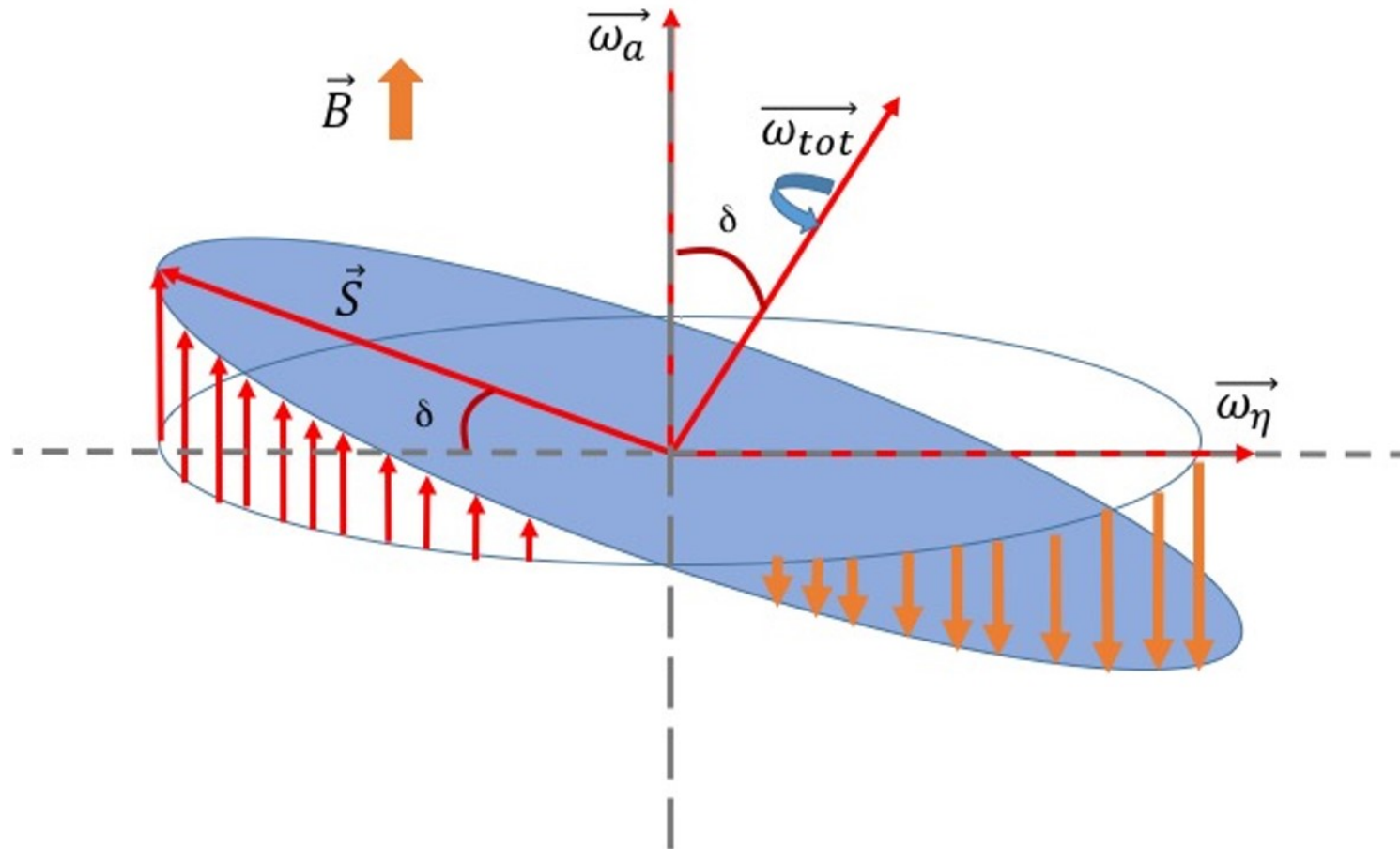
Meeting the TDR goal of 20 ppb.

Projection of Data Acquisition as a Multiple of BNL Data



Currently:
~5xBNL physics
quality data

Future EDM or μ^- anomalous MDM Possibilities



- Currently measuring μ^+ anomalous MDM
- Measure μ^+ EDM using vertical phase asymmetry detection in calorimeters
- Measure μ^- by reconfiguring the beamlines and storage ring (switching electric field direction)
 - No other proposed experiment can do μ^- (JPARC μ^+ only)

- The experiment is running well and has entered Run-3.
- The analysis is coming along, and we are expecting to publish first results this year.
- We have developed sophisticated modeling tools and data-driven approaches to quantify systematics, e.g. the muon loss phase.

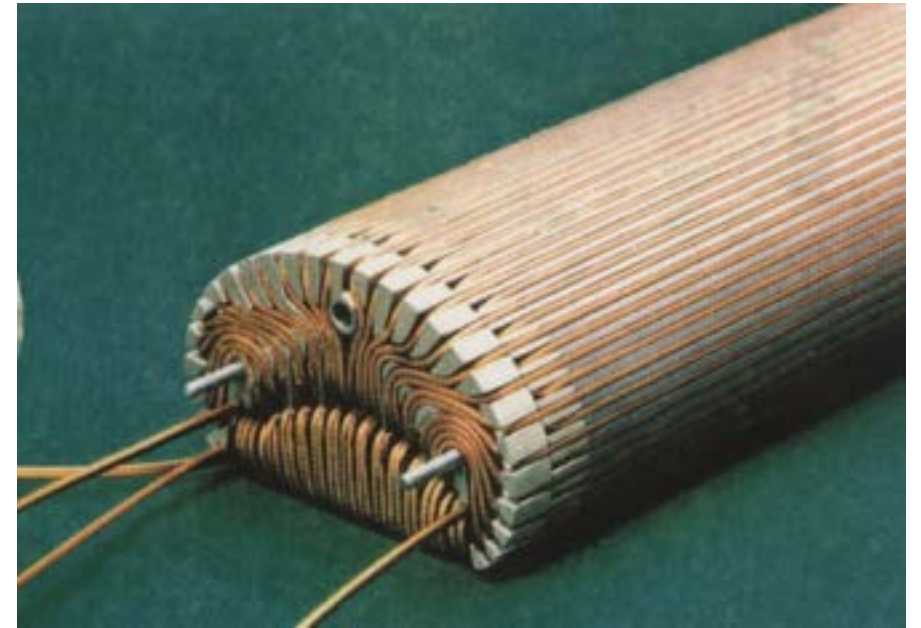
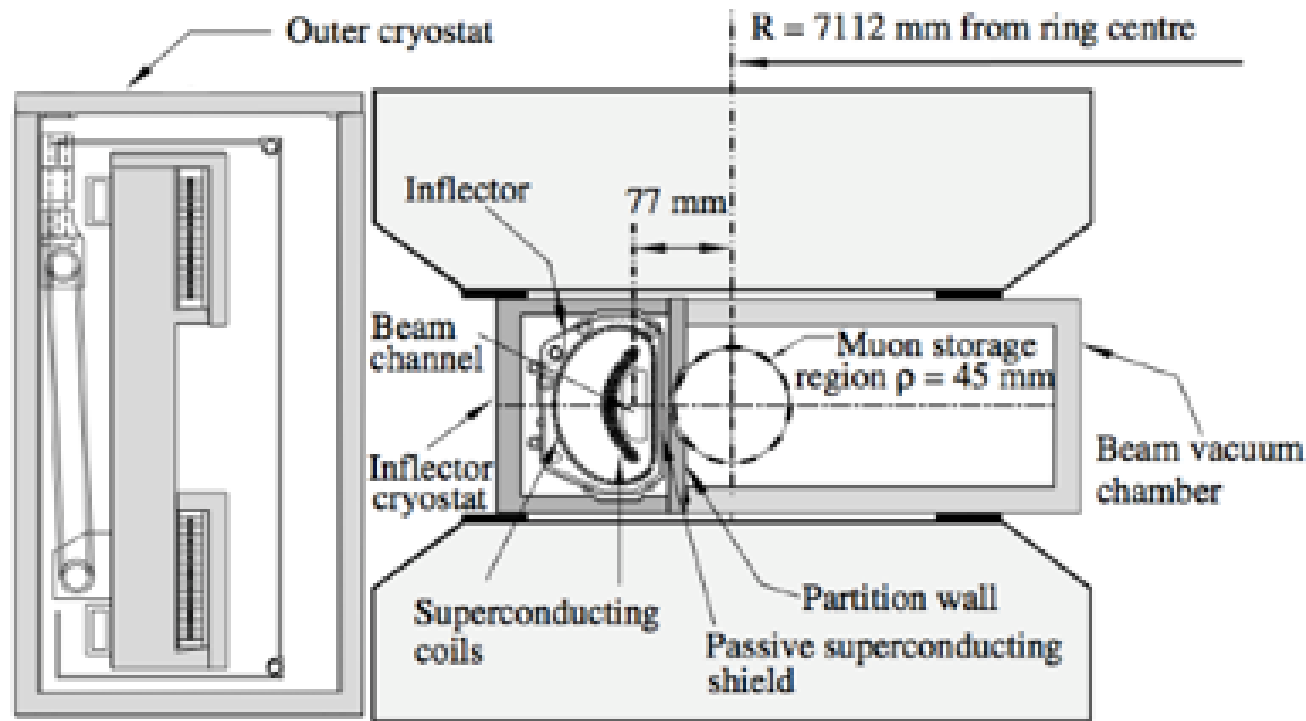


U.S. DEPARTMENT OF
ENERGY

Office of
Science

- This material is based upon work supported by the U.S. Department of Energy, Office of Science, under Contract No. DE-FG02-08ER41546 and Contract No. DE-SC0018636.
- This document was prepared by the Muon g-2 collaboration using the resources of the Fermi National Accelerator Laboratory (Fermilab), a U.S. Department of Energy, Office of Science, HEP User Facility. Fermilab is managed by Fermi Research Alliance, LLC (FRA), acting under Contract No. DE-AC02-07CH11359.
- This research used resources of the National Energy Research Scientific Computing Center (NERSC), a U.S. Department of Energy Office of Science User Facility operated under Contract No. DE-AC02-05CH11231.
- This research was done using resources provided by the Open Science Grid, which is supported by the National Science Foundation award 1148698, and the U.S. Department of Energy's Office of Science.

Muon g-2 Inflector



- 1.45 T bucking field to cancel main field
- Can't perturb main field by more than ~ 1 ppm
- Interface optics of storage ring and the M5 beamline

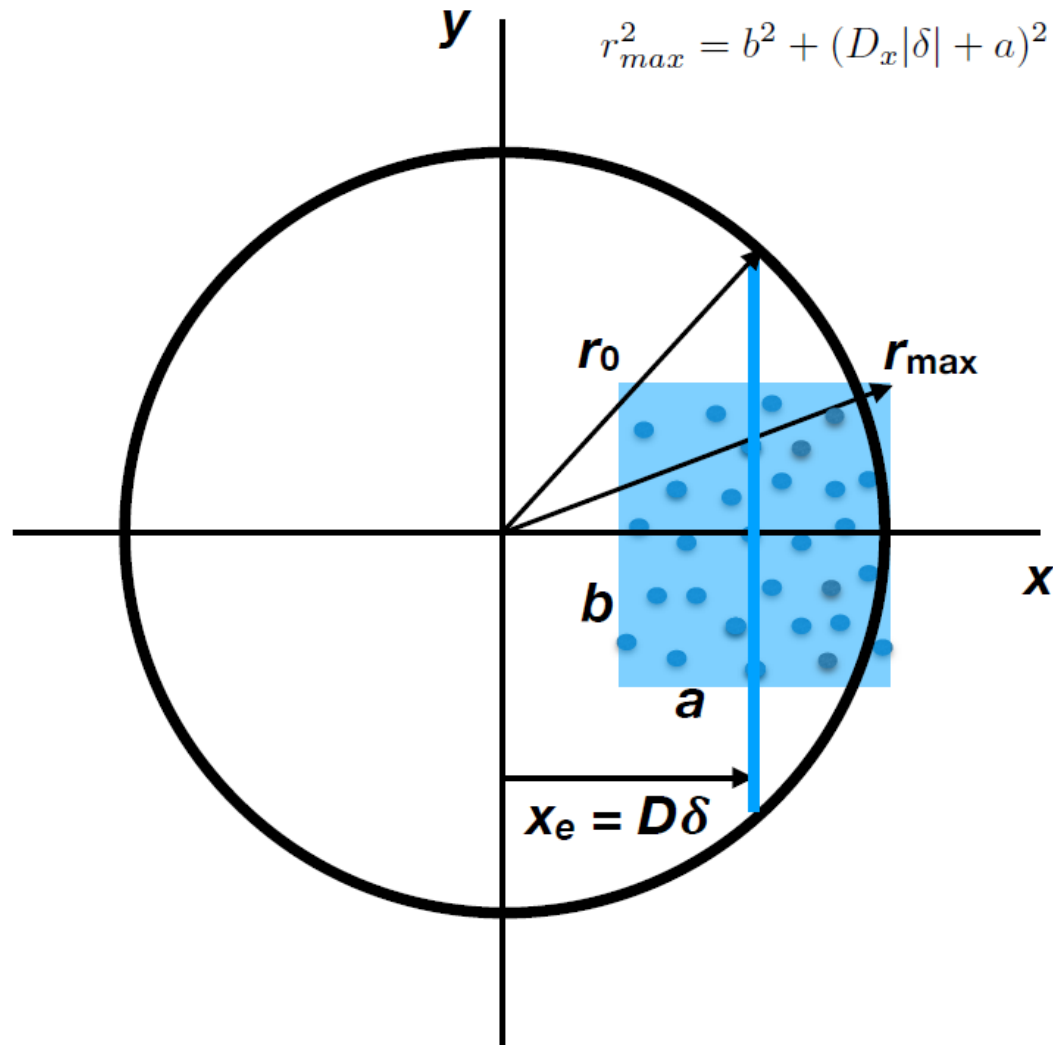
Fitting Function Example: 20 Point

$$N = N_0 \Lambda N_{cbo} N_{2cbo} N_{vw} e^{-t/\tau} (1 - A A_{cbo} \cos(\omega_a t + \phi \phi_{cbo}))$$

$$\begin{aligned} N_{cbo} &= 1 - A_{1cbo} e^{-\frac{t}{\tau_{cbo}}} \cos(\omega_{cbo} t + \phi_{1cbo}) \\ N_{2cbo} &= 1 - A_{2cbo} e^{-\frac{2t}{\tau_{cbo}}} \cos(2\omega_{cbo} t + \phi_{2cbo}) \\ N_{vw} &= 1 - A_{vw} e^{-\frac{t}{\tau_{vw}}} \cos(\omega_{vw} t + \phi_{vw}) \\ A_{cbo} &= 1 - A_{Acbo} e^{-\frac{t}{\tau_{cbo}}} \cos(\omega_{cbo} t + \phi_{Acbo}) \\ \phi_{cbo} &= 1 - A_{\phi_{cbo}} e^{-\frac{t}{\tau_{cbo}}} \cos(\omega_{cbo} t + \phi_{\phi_{cbo}}) \\ \omega_{cbo} &= \omega_0 (1 + 2.875 e^{-\frac{t}{76}} / \omega_0 t + 5.47 e^{-\frac{t}{8.85}} / \omega_0 t) \\ \Lambda &= 1 - K_{loss} \int L(t') e^{t'/64.4} dt \end{aligned} \quad \chi^2 = \sum_{i=1}^{ndf} \left[\frac{N_{bin} - N_{fit}}{\sigma(N_{bin})} \right]^2$$

Momentum-Dependent Muon Losses

Mike Syphers



$$\frac{\Delta\omega_a}{\omega_a} = \frac{1}{\omega_a} \frac{d\langle\Phi\rangle}{d\langle dp/p_0\rangle} \frac{d\langle dp/p_0\rangle}{dt}$$

Straw Tracking Detectors

